







## ORIGINAL ARTICLE OPEN ACCESS

## The Deep-Sea Preyscapes of Mammalian Top Predators

Véronique Merten<sup>1</sup>  | Marie Guilpin<sup>2,3</sup> | Julia M. Parker<sup>1</sup>  | Machiel Oudejans<sup>3</sup> | Shannon M. Dolan<sup>4</sup>  | Simone Baumann-Pickering<sup>4</sup>  | Elliott L. Hazen<sup>5</sup> | Luis M. D. Barcelos<sup>6</sup>  | Miguel Fernandes Guerreiro<sup>7</sup>  | Filipe M. Porteiro<sup>8</sup> | Sören Franzenburg<sup>9</sup> | Till Bayer<sup>1</sup> | Henk-Jan Hoving<sup>1</sup> | Fleur Visser<sup>2,3</sup>

<sup>1</sup>GEOMAR Helmholtz Centre for Ocean Research Kiel, Kiel, Germany | <sup>2</sup>Department of Coastal Systems, NIOZ Royal Netherlands Institute for Sea Research, Texel, the Netherlands | <sup>3</sup>Kelp Marine Research, Heiloo, the Netherlands | <sup>4</sup>Scripps Institution of Oceanography, University of California, La Jolla, California, USA | <sup>5</sup>Department of Ecology and Evolutionary Biology, University of California Santa Cruz, Santa Cruz, California, USA | <sup>6</sup>Azorean Biodiversity Group & cE3c—Center for Ecology, Evolution and Environmental Changes & CHANGE—Global Change and Sustainability Institute, Faculty of Agrarian Sciences and Environment (FCAA), University of the Azores, Angra do Heroísmo, Azores, Portugal | <sup>7</sup>Centre for Environmental and Marine Studies (CESAM), Department of Biology, University of Aveiro, Aveiro, Portugal | <sup>8</sup>Institute of Marine Sciences, OKEANOS, University of the Azores, Horta, Portugal | <sup>9</sup>Institute of Clinical Molecular Biology, Kiel University and University Hospital Schleswig-Holstein, Kiel, Germany

**Correspondence:** Véronique Merten ([vmerten@geomar.de](mailto:vmerten@geomar.de))

**Received:** 18 September 2025 | **Revised:** 7 March 2026 | **Accepted:** 15 April 2026

**Keywords:** cephalopods | cetaceans | deep-sea acoustic backscatter | deep-sea preyscape | deep-sea richness | eDNA | fish

## ABSTRACT

Prey richness, accessibility, and density shape predator foraging strategies. Deep-sea preyscapes, however, remain largely unknown, limiting our understanding of how prey presence and distribution shape predator movement, energy budget, and ecological role. Using combined eDNA metabarcoding and hydroacoustics, we investigated the deep-sea cephalopod and fish preyscapes of three co-occurring cetacean predators (Risso's dolphins (*Grampus griseus*), Sowerby's beaked whales (*Mesoplodon bidens*), and goose-beaked whales (*Ziphius cavirostris*)) across an inshore-offshore gradient. We tested whether (i) prey acoustic backscatter (a metric for density) and taxonomic richness decreased with distance from shore; (ii) predators exploit localized peaks in prey density and richness; and (iii) prey composition and density varied across adjacent foraging habitats along the inshore-offshore gradient. Across 117 samples, we detected 37 cephalopod and 66 fish taxa, including other top predators (sharks). Acoustic backscatter was concentrated within the deep scattering layer (DSL). Yet, peak taxonomic richness occurred above and below it, suggesting that the local DSL holds relatively limited fish and cephalopod richness. The offshore DSLs were vertically shallower and more stable, while the inshore DSL was deeper and bifurcated, possibly due to predator avoidance. Contrary to expectation, acoustic backscatter offshore was up to five-fold higher than inshore, and taxonomic richness did not decrease with distance from shore. Fish communities varied primarily with depth, whereas cephalopod communities varied along the inshore-offshore gradient. Bathypelagic offshore foraging zones of goose-beaked whales contained overall low acoustic backscatter but high taxonomic richness. This suggests that goose-beaked whales may target large, energy-rich cephalopods and prioritize prey quality over density. Our results reveal vertical and horizontal habitat complexity in an oceanic ecosystem that may shape predator–prey interactions and habitat partitioning among cetacean species.

## 1 | Introduction

Predator–prey interactions shape and stabilize ecosystem function, yet our understanding of these dynamics in the deep sea remains limited (Herring 2002; Ramirez-Llodra et al. 2010). This

gap persists despite the deep sea being a vital component of global marine ecosystems (Levin et al. 2019). The deep sea is structured by steep gradients in light, pressure, oxygen, and food resources that govern species' behavior and distributions and, in turn, predator preyscapes (Seibel 2011). The deep sea and the sunlit epipelagic

Véronique Merten and Marie Guilpin should be considered joint first authors.

This is an open access article under the terms of the [Creative Commons Attribution](https://creativecommons.org/licenses/by/4.0/) License, which permits use, distribution and reproduction in any medium, provided the original work is properly cited.

© 2026 The Author(s). *Environmental DNA* published by John Wiley & Sons Ltd.

waters are vertically and ecologically connected, but the extent and specific interactions that underlie this connectivity remain poorly understood. Many fish and cephalopod species have wide distributions and show vertical and horizontal mobility, creating a dynamic preyscape that shapes predator foraging strategies (Sutton et al. 2008). Vertical connectivity between epi- and mesopelagic habitats is further strongly facilitated by diel vertical migration (DVM) (Barham 1966), a widespread behavioral phenomenon in which numerous fish and invertebrate species ascend in the water column at night to feed and descend by day to evade predation, transporting biomass, nutrients, and energy across depth layers (Robinson et al. 2010; Robison 2009).

A key feature of diel vertical migration is the evident deep-scattering layer (DSL). Sound scattering layers are globally distributed, acoustically detectable layers. They are typically located between 200 and 1000 m depth, and composed of dense aggregations of zooplankton and nekton (Barham 1966; Benoit-Bird et al. 2017). The DSL is an important foraging ground for predators, including sharks, other large predatory fish, and marine mammals, effectively linking mesopelagic prey to shallower and deeper habitats (Arostegui et al. 2020; Braun, Lezama-Ochoa, et al. 2023; Braun et al. 2019; Hazen, Jorgensen, et al. 2013; Hazen and Johnston 2010; Josse et al. 1998). Some predators, however, forage beyond the DSL and into the bathypelagic zone to feed (Braun, Della Penna, et al. 2023; Braun et al. 2022; Houghton et al. 2008; Howey et al. 2016; McIntyre et al. 2012; Schorr et al. 2014; Thorrold et al. 2014). The various foraging depths of oceanic predators suggest a structured layering of prey, including the DSL as well as deeper occurrences and aggregations. However, the composition of such prey layers remains undocumented for most regions.

Oceanic islands are oceanic biodiversity and foraging hotspots (Afonso et al. 2020; Morato et al. 2010), where seafloor topography and oceanographic processes such as fronts, eddies, upwelling, and mixing enhance local productivity (Hazen, Suryan, et al. 2013; Scales et al. 2014). These features can lead to localized prey concentration, attracting a range of predators, including dolphins and tuna (Barton et al. 2000; Caldeira et al. 2002; Gove et al. 2016; Schütte et al. 2025, 2015). However, the extent to which island-associated productivity shapes the foraging strategies of deep-diving predators remains poorly understood (Arce et al. 2022; Bailleul et al. 2007; Salvetat et al. 2022; Steinberg et al. 2021). This raises the question of whether nearshore island systems offer more favorable foraging conditions than offshore habitats due to enhanced habitat heterogeneity and prey availability.

Cetacean foraging, including movement patterns and hunting efficiency, is generally driven by prey density and distribution (Friedlaender et al. 2009; Goldbogen et al. 2015; Watanabe et al. 2014). Deep-sea forage species span a wide taxonomic breadth, but two nekton groups stand out in their calorific and numerical importance: cephalopods and fishes. Cephalopods appear in the diets of at least 90% of whale species and serve as the primary food source in at least 42% (Clarke 1996; Spitz et al. 2011). In addition, mesopelagic fish such as myctophids (lanternfish) also constitute a critical component of the diet of many cetaceans foraging in the pelagic realm (Barlow et al. 2008). The high energy demands of warm-blooded deep-diving predators suggest the existence of substantial deep-sea

biomass with energy-rich prey. For instance, sperm whales (*Physeter macrocephalus* Linnaeus, 1758) alone are estimated to consume a biomass of ~110 (96–320) million tons of cephalopods annually (Clarke 1977). Above the Mid Atlantic Ridge, bathypelagic fish biomass near the seafloor may even exceed mesopelagic biomass (Sutton et al. 2008), suggesting significant prey resources at deeper depths (Kaartvedt et al. 2020; Sutton 2013). It remains unclear which characteristics of deep-sea preyscapes provide suitable foraging conditions for oceanic top predators and whether they are drawn to areas of greater prey diversity, increased abundance, or other ecological factors.

Here, we investigate the biological characteristics of the foraging zones used by three cetacean top predators (Risso's dolphins *Grampus griseus* (G. Cuvier, 1812), Sowerby's beaked whales *Mesoplodon bidens* (Sowerby, 1804), and goose-beaked whales *Ziphius cavirostris* (Cuvier, 1823)) to identify the preyscape characteristics contributing to suitable foraging habitats. We integrate hydroacoustic data with environmental DNA (eDNA) metabarcoding to investigate the influence of nektonic prey availability, biomass, and distribution on the foraging habitat selection of these three cetacean species. The combination of these methods has been previously used to characterize pelagic forage fish in a whale feeding area (Berger et al. 2020), to investigate diel vertical migration in the Gulf of Mexico (Easson et al. 2020), and to show a positive correlation between eDNA fish concentration and backscatter intensity around artificial reefs (Sato et al. 2021). These complementary methods enable us to link broad-scale acoustic backscatter estimates, a proxy for density, with fine-scale taxonomic identification of the contributing organisms. This approach will allow quantification of prey richness and distribution across depth strata and analysis on how deep-sea preyscapes may influence top predator foraging strategies. We hypothesize that (i) prey acoustic backscatter (a metric for density) and taxonomic richness decrease with increasing distance from shore; (ii) predators exploit localized peaks in density and taxonomic richness; and (iii) preyscape (prey composition and density) varies across foraging habitats, resulting in distinct prey fields across habitats.

## 2 | Material and Methods

Field sampling was conducted off Terceira Island, Azores, where three deep-diving cetacean species, Risso's dolphins, Sowerby's beaked whales, and goose-beaked whales, are known to use distinct foraging habitats along an inshore-offshore gradient (predator core habitat areas, Figure 1). Environmental DNA (eDNA) and hydroacoustic data were collected at three stations representing these habitats (Figure 1). This matched sampling design enabled the characterization of prey richness and acoustic backscatter (a metric for density) across depth and habitat zones relevant to each predator species. Risso's dolphins forage inshore, Sowerby's beaked whales at intermediate distances to shore, and goose-beaked whales offshore (Visser, Merten, et al. 2021, Sowerby's beaked whale distribution: personal communication with F. Visser). In addition, Risso's dolphins forage at shallower depths between 200 and 600 m in comparison to Sowerby's and beaked whales foraging at deeper depths between 900 m and the seafloor (Visser et al. 2022; Visser, Keller, et al. 2021; Visser, Merten, et al. 2021).

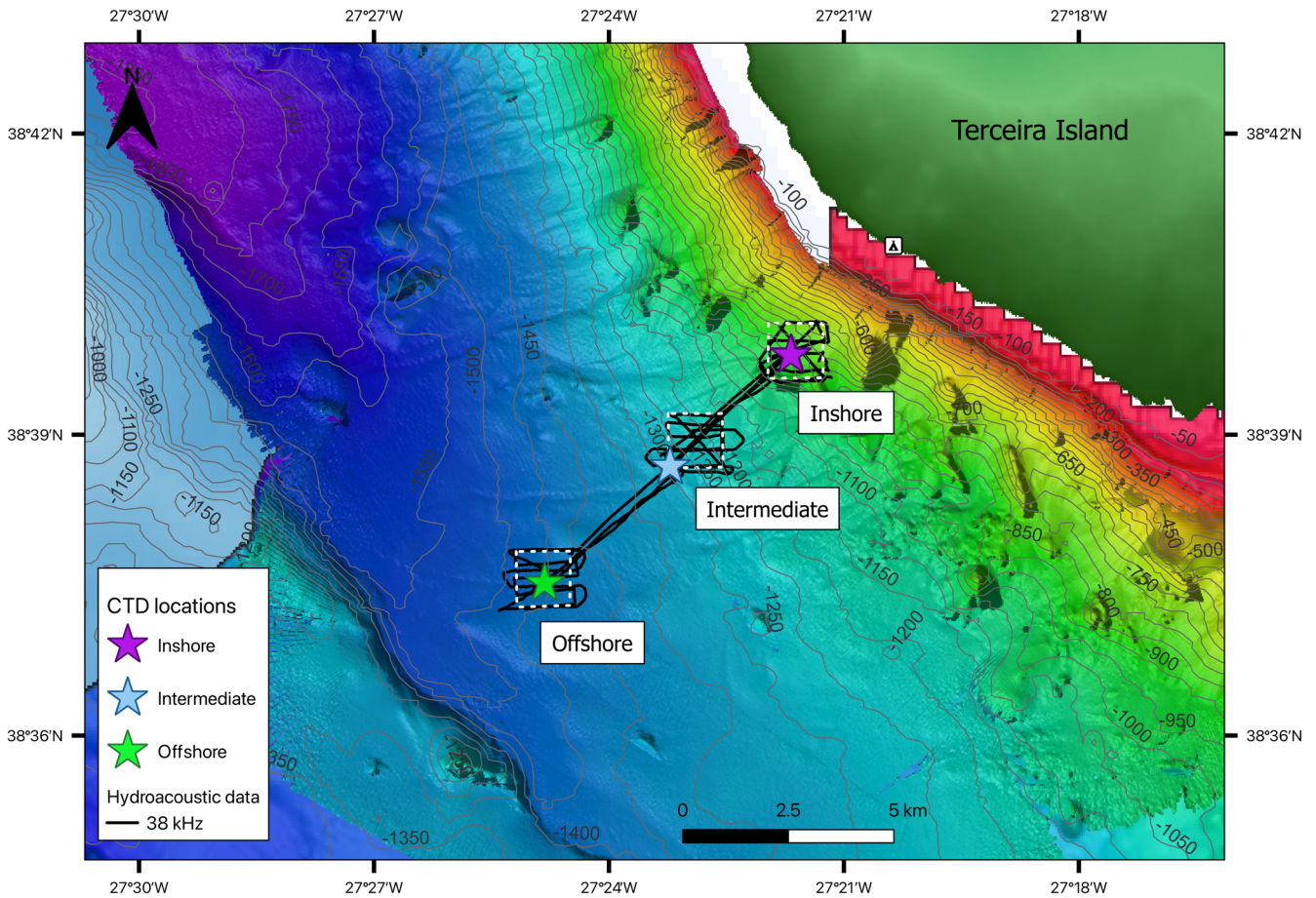


**FIGURE 1** | Study design. Research area off Terceira Island, Azores, showing spatial overlap among daylight systematic hydroacoustic transects (solid lines), predator core foraging habitat areas (white dashed squares), and eDNA sampling locations (by CTD-rosette (CTD = Conductivity, Temperature and Depth) depicted by the colored stars). Inshore: Foraging habitat of Risso's dolphins; Intermediate: Foraging habitat of Sowerby's beaked whales; Offshore: Foraging habitat of goose-beaked whales. Bathypelagic acoustic data were collected from a mooring deployed at the goose-beaked whale CTD site (green star). Bathymetry from multibeam NIOZ data. Map created in QGIS v. 3.16.6 (QGIS Development Team, 2021).

## 2.1 | Environmental DNA Processing and Analysis

### 2.1.1 | Sample Collection, Filtration, and Environmental DNA Extraction

In 2021, on board the *R/V Pelagia* (64PE488), water samples were taken using a CTD-rosette (CTD = Conductivity, Temperature and Depth) with attached Niskin bottles at known foraging locations of Risso's dolphins (inshore, 50–800 m depth), Sowerby's beaked whales (intermediate, 50–1288 m depth), and goose-beaked whales (offshore, 50–1446 m depth) (Figure 1). At the intermediate and offshore stations, two CTD casts were required, one for the upper 800 m and a second to reach the remaining depths down to the seafloor. Samples were collected at 50 and 100 m and then in 100 m depth intervals until above the bottom throughout the water column within each foraging habitat, resulting in 9 depths sampled inshore, 14 depths at intermediate distance from the island, and 16 depths offshore (each depth in triplicate, 117 samples in total). Niskin bottles, which remained open during descent and hence are continuously flushed with ambient seawater, were closed after a pause of several minutes at the target depth to minimize contamination from overlying water layers. For each depth, 2 L of seawater were directly filtered from a CTD Niskin bottle using sterile tubing onto a

0.22  $\mu\text{m}$  GP Sterivex filter in pseudo-triplicates. To control for deck contamination, a blank filter was collected at each station by filtering 500 mL of MilliQ water. All filters were sealed and stored at  $-80^{\circ}\text{C}$  until further processing.

In the laboratory, the DNA from the filters was extracted following a modified version of the Qiagen DNeasy Blood and Tissue kit (Visser, Merten, et al. 2021). Briefly, after thawing for 12 h at  $4^{\circ}\text{C}$ , the outside of each filter capsule was wiped with RNase Away decontamination reagent. 720  $\mu\text{L}$  ATL-buffer and 80  $\mu\text{L}$  proteinase K were added directly to the filter and incubated for 16–18 h at  $56^{\circ}\text{C}$  in a rotating oven. After incubation, the buffer mix was transferred to a sterile 2 mL Eppendorf tube. From each sample, 600  $\mu\text{L}$  was pipetted to a new 2 mL Eppendorf tube and afterwards mixed with 600  $\mu\text{L}$  AL-Buffer and 600  $\mu\text{L}$  99% ethanol high grade. The next steps were followed as described in the DNeasy Blood and Tissue protocol. Lastly, DNA was eluted in 70  $\mu\text{L}$  pre-warmed AE-Buffer.

### 2.1.2 | Library Preparation and Sequencing

To detect the presence of cephalopod eDNA in all samples, two cephalopod specific primer sets were used. The

first targeted the cephalopod specific nuclear 18S rRNA V2 region, producing an amplicon of approximately 160bp (Ceph18S\_forward 5'-CGCGGCGCTACATATTAGAC-3' and Ceph18S\_reverse 5'-GCACTTAACCGACCGTTCGAC-3') (de Jonge et al. 2021). The second primer targeted the mitochondrial 16S rDNA gene, yielding an amplicon of approximately 230bp (CephMLSf1 TGGCGTATTWTAAGTACT and CephMLSr1 TTATTCCTTRATCACCC) (Jarman et al. 2006). To detect the presence of fish eDNA, a fish specific primer targeting the mitochondrial 12S rRNA gene was used, yielding an amplicon of approximately 100bp (teleo\_12S\_forward ACACCGCCCCGCTACTCT, teleo\_12S\_reverse CTTCCGGTACTTACCATG) (Valentini et al. 2016). Both the Ceph18S and teleo\_12S primers were used in a one-step PCR protocol, in which Illumina index primers with unique adapters were already attached to the primer sequence. In contrast, a two-step PCR protocol was used for the CephMLS primer: the first PCR amplified the target DNA, and the second PCR incorporated the Illumina index primers. In both library preparation approaches, combinatorial dual indexing was employed, whereby unique combinations of i5 and i7 index primers were used to distinguish samples within the sequencing run.

The one-step-PCRs for Ceph18S and teleo\_12S had a total volume of 25  $\mu$ L and included 10  $\mu$ L of Taqman environmental Mastermix 2.0 (ThermoFisher), 8  $\mu$ L of PCR-grade water, 1  $\mu$ L of the forward and reverse primers each (Ceph18S: 5  $\mu$ M; teleo\_12S: 2.5  $\mu$ M) and 5  $\mu$ L of the DNA template. The PCR cycling conditions for Ceph18S were as follows: initial denaturation step at 95°C for 10 min, followed by 8 cycles of a touchdown PCR (94°C for 30s, 70°C–1°C after each cycle for 30s, 72°C for 1 min). The PCR was continued with 32 cycles of 94°C for 30s, annealing at 62°C for 30s, and extension at 72°C for 1 min and terminated after a final extension step at 72°C for 5 min. The PCR cycling conditions for teleo\_12S were as follows: initial denaturation step at 95°C for 10 min, followed by 40 cycles of 94°C for 30s, annealing at 55°C for 30s and extension at 72°C for 1 min. The PCR was terminated after a final extension step at 72°C for 5 min.

The first PCR for CephMLS had a total volume of 25  $\mu$ L and included 11  $\mu$ L of 2 $\times$  KAPA HiFi HotStart Ready Mix, 6  $\mu$ L of PCR-grade water, 1  $\mu$ L DMSO, 1  $\mu$ L of the forward and reverse primers with adapter (CephMLS: 5  $\mu$ M) and 5  $\mu$ L of DNA template. The cycles for the first PCR were as follows: initial denaturation step at 95°C for 5 min, followed by 35 cycles of 98°C for 20s, annealing at 55°C for 15s and extension at 72°C for 1 min, followed by a final cycle of 72°C for 10 min. Prior to the second PCR, all technical replicates were pooled and diluted 1:10 with PCR-grade water. The mastermix for the second PCR had a total volume of 10  $\mu$ L, containing 1  $\mu$ L of PCR-grade water, 2.5  $\mu$ L of 2 $\times$  KAPA HiFi HotStart Ready Mix, 0.5  $\mu$ L DMSO and 0.5  $\mu$ L of each unique combination for each sample of forward and reverse Illumina Index Primers (5  $\mu$ M). Lastly, 5  $\mu$ L of 1:10 diluted template from the first PCR was added. The PCR program for the second PCR was as follows: initial denaturation step at 95°C for 5 min, followed by 10 cycles of 98°C for 20s, annealing at 55°C for 15s and extension at 72°C for 1 min, terminated by a final cycle of 72°C for 10 min.

Fragment sizes were confirmed using a 2% agarose gel stained with GelRed (Biotium). PCR triplicates were pooled, quantified

with the Qubit dsDNA HS Assay Kit (Molecular Probes, Life Technologies) and pooled at equimolar concentrations before undergoing gel purification with the ZymoClean Gel DNA Recovery Kit (Zymo Research Europe). Next-Generation Sequencing was conducted at the Competence Centre for Genomic Analysis (CCGA) in Kiel, Germany. Insert size distribution was assessed using the 4200 TapeStation D5000 ScreenTape (Agilent). The working solution was diluted to 2 nM, and the loading solution was prepared according to protocol. Library pools were loaded at 8 pM with a 20% PhiX spike-in to enhance diversity. Sequencing was performed on an Illumina MiSeq using the MiSeq Reagent Kit v3 (2 $\times$ 300bp) for Ceph18S and CephMLS and v2 for teleo\_12S (2 $\times$ 150bp).

### 2.1.3 | Contamination Controls

To control for deck contamination on the research vessel, a blank filter was collected at each station by filtering 500 mL of MilliQ water and stored together with the eDNA filters.

In the laboratory, to reduce the risk of contamination from foreign DNA or cross-contamination between samples, each filter and tube was treated individually, never opening more than one at a time, and all laboratory steps were conducted under separate clean benches and laboratories. The same holds true for library preparation, where each sample was pipetted individually. To control for contamination in the laboratory, per primer and on every 96-well plate, one negative control (PCR-grade water), two positive controls and one mock control (1:1 mix of positive controls) were added. DNA used for positive controls derived from species that do not occur in the North Atlantic (*Filippovia knipovitchi* (Filippova, 1972) and *Psychroteuthis glacialis* (Thiele, 1920), for both cephalopod primers and *Danio rerio* (Hamilton, 1822) and *Oncorhynchus clarkii* (Richardson, 1836) for the fish primer). Every sample was amplified in PCR-triplicates, pooled after PCR and sequenced together with the eDNA samples.

### 2.1.4 | Bioinformatic Analysis of Environmental DNA Data

Following sequencing, the obtained reads were demultiplexed by the sequencing center. The PCR primers were removed utilizing cutadapt (version 1.18; (Martin 2011)). Only sequences containing both the forward and reverse primer were retained for subsequent analysis employing DADA2 (version 1.16.0; (Callahan et al. 2016)). The sequences underwent filtration based on specific criteria: those containing Ns were eliminated (maxN=0), and sequences were truncated upon encountering the first instance of a quality score of 2 or lower (truncQ=2). Additionally, sequences exhibiting an expected error exceeding 3 for forward reads and 5 for reverse reads were removed (maxEE=3,5). A comparatively higher expected error threshold was applied to the reverse reads due to their generally lower quality compared to the forward reads. Subsequently, forward and reverse reads were merged, requiring a minimum overlap of at least 80bp for cephalopods and 20bp for fish, and chimeras were removed.

For cephalopods, taxonomic assignments for both samples and controls adhered to the methodology outlined in Merten

et al. (2021). To summarize, sequences of cephalopods sourced from the SILVA 18S database were cross-referenced with the NCBI GenBank database until no additional cephalopod sequences were identified, resulting in a collection of 169 sequences spanning 119 species. Subsequently, a reference database for cephalopods was constructed by combining these sequences with all other eukaryotic 18S rRNA sequences from the SILVA database, thereby mitigating the risk of erroneous assignments of non-cephalopod amplicons. As for fishes, taxonomic assignments were facilitated using the MIDORI 2 database comprising 12S gene sequences derived from NCBI GenBank release 248 (Leray et al. 2022). The provided files underwent reformatting to ensure compatibility with the IDTAXA program (Murali et al. 2018). Non-marine species were removed from the full dataset prior to downstream analysis. For each type of control sample (negative, filtration, or extraction controls), the maximum amplicon sequence variant (ASV) read count observed for each negative control type was subtracted from the corresponding ASV across the associated samples. Following this correction, ASVs represented by fewer than 10 reads were removed from the dataset.

### 2.1.5 | Statistical Analysis of Environmental DNA Data

The statistical analysis was conducted in R (version: 4.4.1; (R Core Team 2021)). All analyses were conducted using presence/absence data, which provides a robust representation of taxa occurrence. Abundance estimates derived from eDNA are affected by PCR amplification biases, stochasticity, and marker-specific detection efficiencies (Kelly et al. 2019). Therefore, we did not perform corrections on the sequencing read count data, and did not infer abundance or biomass estimates of taxa.

To facilitate comparison across depth strata, sampling depths were binned into two habitat zones: shallow (0–800m water depth) and deep (900m to bottom). The nearshore station (max. depth 800m; shallow) represents the epi- and mesopelagic, which is connected through diel vertical migration and harbors the deep-scattering layer. The two deeper offshore stations (max. depths 1200 and 1450m; shallow and deep) represent meso- and bathypelagic waters. In order to investigate whether statistically significant differences between the different depth bins existed, a Jaccard index matrix was created to construct nonmetric multidimensional scaling (NMDS) plots using the package *vegan* with the function “metaMDS” (Oksanen et al. 2019), followed by a permutational multivariate analysis of variance (PERMANOVA) using distance matrices with the function “adonis” (package *vegan*). When the PERMANOVA was significant, we used the package *pairwise.adonis* (Martinez 2020) to indicate which habitat was significantly different. The area-proportional Euler diagrams showing shared and distinct taxa communities were created with the package *eulerr* (Larsson and Gustafsson 2018). To assess differences in taxa richness across habitat zones, we calculated taxa richness from the presence/absence community matrix using the “specnumber” function (*vegan* package). Prior to conducting parametric tests, we verified that the assumptions for ANOVA were met. Homogeneity of variances was tested using Levene’s test with the function “leveneTest” (package *car*) (Fox and Weisberg 2019). Normality of residuals was assessed using the Shapiro–Wilk test with the function “shapiro.test” (*stats* package). We then performed a one-way ANOVA to test for differences in taxa richness

across five zonation categories controlling for the differences in sampling effort per category (“aov”). Post hoc pairwise comparisons were conducted using Tukey’s Honest Significant Difference test using the function “TukeyHSD” (*stats* package). Species accumulation curves were generated separately for each habitat zone (inshore, intermediate, offshore) and for both taxonomic groups (fish and cephalopods) using the “specaccum” function (*vegan* package), providing an estimate of how species richness increases with sampling effort. For each group, the curves display the mean accumulated richness across sampling depths, along with standard deviation. The rarefaction curves were generated with the *vegan* package “rarecurve” displaying the sequencing depth per sample.

## 2.2 | Hydroacoustic Data

### 2.2.1 | Hydroacoustic Data Collection and Processing—Surface-Mounted Echosounders

Hydroacoustic data were collected during surveys on R/V *Pelagia* and R/V *Nephtin* in June and August 2021, respectively. Data were recorded continuously aboard R/V *Pelagia* with Simrad EK60 echosounder operating at 38 kHz during both systematic and stationary sampling, that is simultaneously to eDNA collection. Daytime systematic surveys were performed in August 2021 (R/V *Nephtin*) using a Simrad EK60 (38 kHz) frequency echosounder (max bottom depth 1500 m). The echosounder systems were field calibrated according to standard procedures (Demer et al. 2015; Foote et al. 1987) using a 38.1 mm tungsten carbide sphere and suspended 3–4 m below the transducers. Systematic transects were focused on defined habitat boxes for each of the three deep-diving predators and the inshore-offshore gradient between these boxes (Figure 1). The acoustic backscatter was sampled at a maximum ping rate with pulse duration of 0.512 and 1.024 ms for the systems on R/V *Pelagia* and R/V *Nephtin*, respectively, which were used to measure scattering volume backscatter strength  $S_v$  (dB re  $\text{m}^2\text{m}^{-3}$ ) and Nautical Area Scattering Coefficient  $S_A$  (NASC— $\text{m}^2\text{nmi}^{-2}$ ).

Hydroacoustic data from systematic surveys were processed using Echoview 11.1 and Echoview 12.1 (Echoview Software Pty Ltd., Hobart, Australia). The surface layer (0–5 m) was removed to avoid the near-field effects. Data were also processed to eliminate noise from seabed reflections. The data were visually cleaned for unreliable backscatter, non-biological backscatter from over-the-side instrumentation, or missed pings. A horizontal median filter (9×9 pings) was applied to smooth the data. Echo-integration of the data was computed by bins of 50 m on the horizontal axis and by 10 m on the vertical axis.  $S_v$  and  $S_A$  values were exported for the 38 kHz data. Further processing of the hydroacoustic data was done in R (version 4.2.3; (R Core Team 2021)). Time of day, according to location, time, and date, was added using the R package *suncalc* (Thieurmél and Elmarhraoui 2024). We limited the hydroacoustic data to daylight hours. Backscatters above an  $S_v$  threshold of  $-78$  dB re  $1 \text{ m}^2 \text{ m}^{-3}$  were retained, representing sufficiently densely aggregated backscatter (Cade and Benoit-Bird 2014). Bathymetry and distance from shore to the land station reference point (Figure 1) were processed and calculated in the free and open source QGIS (version 3.16.6) for each bin location.

During each CTD cast, hydroacoustic data were concurrently recorded. For broadscale comparisons, averages of  $S_v$  and  $S_A$  were calculated for each CTD cast and then for each CTD location. The volume backscattering coefficient ( $s_v$  in  $\text{m}^2\text{m}^{-3}$ ) was used to calculate  $S_v$  averages and was derived from its logarithmic form, the volume backscattering strength ( $S_v$  in dB re  $\text{m}^2\text{m}^{-3}$ ). It was then converted back to  $S_v$  after averaging.

$$s_v = 10^{(S_v/10)}$$

$$S_v = 10 \times \log 10(s_v)$$

Transects were performed in predator core foraging habitat areas (including CTD casts) and along an inshore-offshore gradient that intersected these areas. Averages of  $S_A$  and  $S_v$  were calculated as described above for each recording period per predator core foraging habitat area or transect section, and then per location.

### 2.2.2 | Statistical Analysis of Hydroacoustic Data—Surface-Mounted Echosounders

In order to assess whether acoustic backscatter in the deep scattering layer varied between the three predator habitats, differences in NASC values were quantified using Generalized Estimating Equations (GEEs; (Hardin and Hilbe 2002)). The sum of NASC across the entire water column and in reference to distance from shore was calculated for each recording bout, and subsequently the mean of the sum of NASC per habitat box ( $n = 5$  inshore,  $n = 6$  intermediate,  $n = 7$  offshore habitat). The sum of NASC in each foraging habitat was modeled as a Gaussian response variable against the factor covariates for *habitat boxes* (inshore, intermediate, offshore). Models were run using the robust variance estimator (Zorn 2006), and using the independence correlation structure to account for spatial autocorrelation. Model selection was performed using a hypothesis-based backwards ANOVA (sequential Wald test). The GEE analyses were run using the package *geepack* (Højsgaard et al. 2005) in R (version 4.2.2; (R Core Team 2021)).

We expected to find a significant effect of “habitat” if acoustic backscatter in the top 800 m was different among the three predator foraging zones. We determined the significance of differences between pairs of conditions (e.g., inshore vs. intermediate habitat) using the  $p$ -values for differences between “habitat boxes” factor levels generated by the final GEE model.

### 2.2.3 | Hydroacoustic Data Collection and Processing—WBAT

An upward-facing Simrad Wideband Autonomous Transceiver (WBAT; Kongsberg, Horten, Norway) echosounder was deployed on a mooring at the goose-beaked whale CTD location (Figure 1). The WBAT was deployed at 1410 m depth and included a split-beam ES70-18CD transducer. The WBAT transmitted a 70 kHz continuous wave pulse with a duration of  $512 \mu\text{s}$  and a ping interval of 4 s. It operated at a duty cycle of emitting 8 pings (32 s total) every 30 min. Data from a March

2021 pool calibration with a 38.1 mm tungsten carbide sphere suspended beneath the WBAT and transducer system was used for calibration. Although the calibration could not be completed in situ at the deployment depth, comparison studies of echosounders at varying depths and environmental conditions show minimal impact on the calibration results (Haris et al. 2018).

The 70 kHz continuous wave WBAT data was processed using Echoview 14.0.227 (Echoview Software Pty Ltd., Hobart, Australia). To avoid near-field effects, data from the first 0–10 m (i.e., 1410–1400 m) from the upward-facing transducer was excluded from the analysis. To ensure positioning of the upward-facing moored WBAT, the Echoview platform settings were adjusted to a fixed heading and the transducer geometry set to  $165^\circ$ , with  $180^\circ$  representing an upward-facing position. The transducer was positioned at a 15-degree offset from the mooring line to prevent noise from other instrumentation on the mooring line in the acoustic beam. The  $z$ -vertical offset was set to 1412 m, corresponding to the depth of the WBAT transducer and calculated from a SBE-37 ODO MicroCAT (Sea-Bird Electronics Inc., Bellevue, WA, USA), located  $\sim 50$  m above the WBAT transducer. It also collected pressure, temperature, and salinity data every 60 s throughout the deployment. Average values for temperature, salinity, and depth were used to calculate a Chen-Milero sound speed velocity, which was applied to the deployment data. Passive pings were removed for analysis by thresholding and matching ping times. The Echoview operators' Background noise removal (De Robertis and Higginbottom 2007), Transient noise removal, and Impulse noise removal (Ryan et al. 2015) were applied to the data. A minimum and maximum volume backscattering strength was set to  $-80$  to  $-60$  dB re  $\text{m}^2\text{m}^{-3}$  to retain putative prey signals, focused on weak-scattering fluid-filled organisms such as squid (Benoit-Bird and Lawson 2016; Campanella et al. 2021; Grassian et al. 2023; Stanton et al. 1987). Nautical Area Scattering Coefficient (NASC) and volume backscatter ( $S_v$ ) values were calculated and exported for a depth range of 1400–1000 m from the cleaned volume backscatter echogram in 5-m and 1-h bins. The moored WBAT collected backscatter data throughout a year-long deployment; however, to temporally match the WBAT data to the eDNA and vessel hydroacoustic data, we present concurrent data from only five days being June 8–10, 2021, and August 2 and 4, 2021.

## 3 | Results

### 3.1 | Water Column Profile

Vertical water column profiles of temperature, salinity, and dissolved oxygen (Figure 2) were similar across the three habitats associated with Risso's dolphins, Sowerby's beaked whales, and goose-beaked whales. Temperature decreased steadily with depth from approximately  $19^\circ\text{C}$  at the surface to  $6^\circ\text{C}$  at 1450 m, with little variation among habitats. Salinity decreased with depth from 36.1 PSU at the surface to 35.2 PSU at depth, again showing no marked differences between habitats. Dissolved oxygen concentrations decreased from 5.4 mL/L at the surface to a minimum of 4.2 mL/L at 800 m depth. In the offshore habitats, the dissolved oxygen increased again below 800 m, reaching

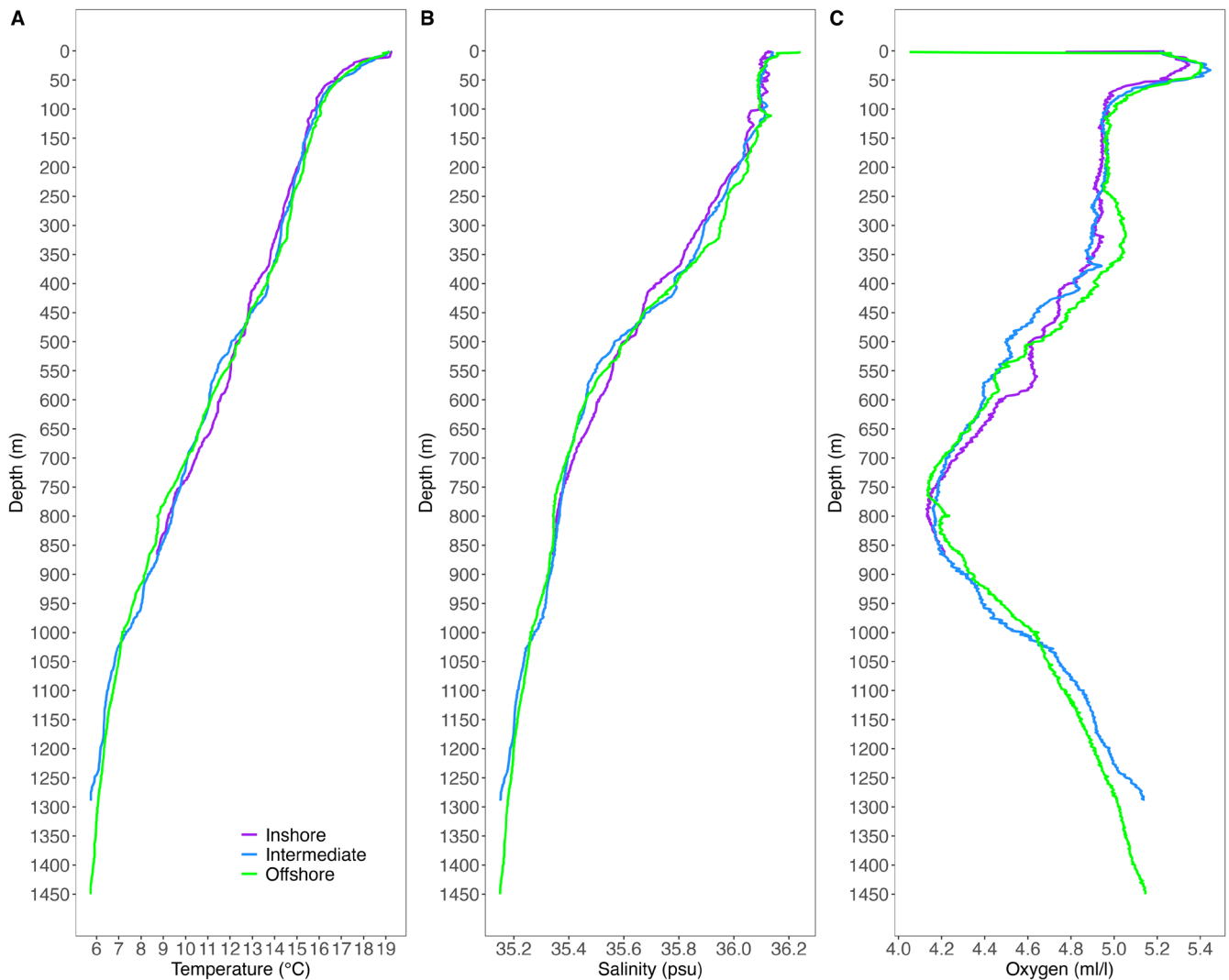


**FIGURE 2** | Vertical profiles of temperature (A), salinity (B), and dissolved oxygen concentration (C) within the water column along an inshore-offshore gradient. Inshore: Risso's dolphin (*Grampus griseus*) foraging habitat; Intermediate: Sowerby's beaked whale (*Mesoplodon bidens*) foraging habitat; Offshore: goose-beaked whales (*Ziphius cavirostris*) foraging habitat.

concentrations of 5.2 mL/L above the seafloor, similar to that of the surface layer. No oxygen minimum zone was observed (values < 0.5 mL/L).

### 3.2 | Sequencing Depth and Amplicon Sequence Richness

The Illumina MiSeq paired-end sequencing of cephalopods resulted in 24.6M and 13.1M sequences with a mean ( $\pm$  SD) of 68.8k (88.4k) and 39.1k (46.7k) reads per sample for the primers CephMLS and Ceph18S, respectively (Table A1). For fish, a total of 10.2M sequences were obtained with a mean of 28.7k (19.0k) reads per sample. The number of sequences in the negative controls was 1433 for CephMLS, 67,316 for Ceph18S and 65,584 for fish (excluding human DNA). After DADA2 analysis, 46.96k and 1.95M sequences remained that were classified into 14 and 279 amplicon sequence variants (ASVs) for CephMLS and Ceph18S, respectively. For fish, 961,968 sequences were classified into 132 ASVs.

### 3.3 | Hydroacoustic Data

A total of 4h and 44min of stationary hydroacoustic data were collected during eDNA collection (48min at the inshore CTD location, 114min at the intermediate CTD location and 121min at the offshore CTD location). A total of ~6h (32 km) of underway hydroacoustic data were collected for the inshore-offshore gradient, ~8h (16km) in the inshore habitat, 7h (15km) in the intermediate habitat, and ~19h (32km) in the offshore habitat.

### 3.4 | Taxonomic Composition of Cephalopod and Fish Environmental DNA

Overall, 37 cephalopod taxa were detected (Figure 3, Tables A2 and A6), of which 65% could be identified to species ( $n = 24$ ), 19% to genus ( $n = 7$ ), and 16% ( $n = 6$ ) to family level. In total, 38% of cephalopod taxa ( $n = 14$ ) were found across all three foraging habitats. The offshore habitat constituted the highest number of unique cephalopod taxa as well as fish

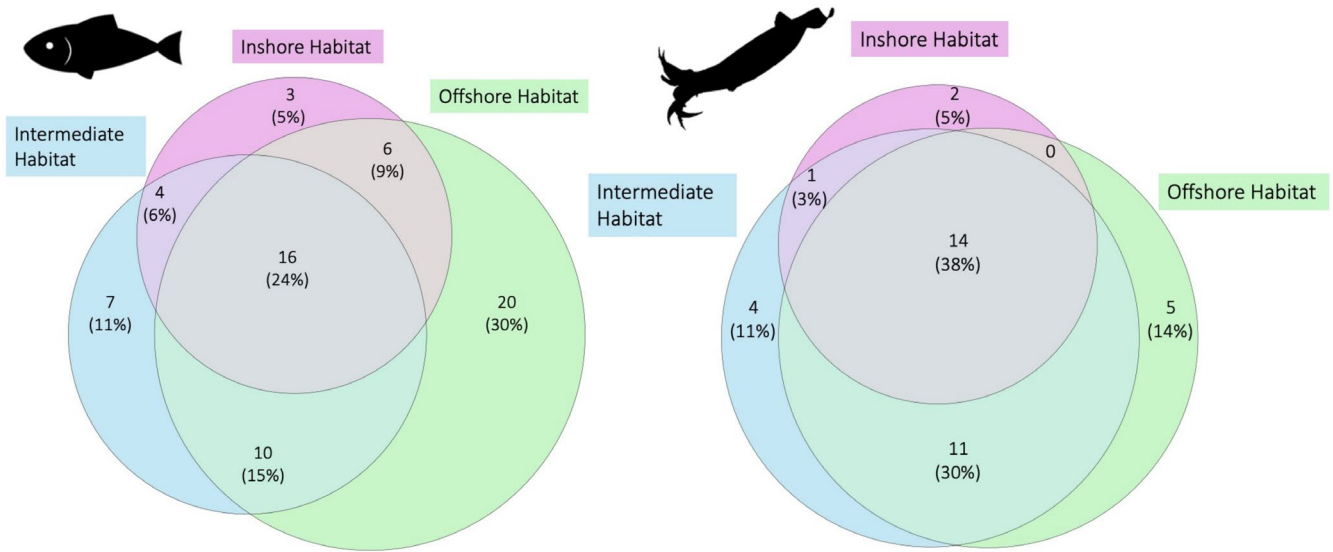


**FIGURE 3** | Inshore-offshore fish (left) and cephalopod (right) community composition detected via eDNA along an inshore-offshore gradient in the foraging habitats of three cetacean top predators. The area-proportional diagram illustrates both shared and habitat-specific fish and cephalopod communities. Inshore habitat = Risso's dolphin (*Grampus griseus*) foraging habitat; Intermediate habitat = Sowerby's beaked whales (*Mesoplodon bidens*) foraging habitat; Offshore habitat = goose-beaked whales (*Ziphius cavirostris*) foraging habitat.

taxa with 14% ( $n = 5$ ) and 30% ( $n = 20$ ) of the community, respectively (Figure 3). For cephalopods, *Heteroteuthis* sp. and *Heteroteuthis dispar* (Rüppell, 1844), with frequencies of occurrence of 71% and 58% across the 38 samples, respectively, were the most often detected taxa, followed by *Idioteuthis magna* (Joubin, 1913) (53%), *Vampyroteuthis infernalis* (Chun, 1903) (53%), *Histioteuthis* sp. (50%), Onychoteuthidae (42%) and *Histioteuthis reversa* (A. E. Verrill, 1880) and Loliginidae with both 32%. All other detections were represented in < 30% of the samples (Figure A1).

A total of 66 fish taxa were detected (Figure 3, Tables A3 and A7), of which 73% were classified to species ( $n = 48$ ), 15% to genus ( $n = 10$ ), and 12% to family level ( $n = 8$ ). All three habitats had 24% of fish taxa ( $n = 16$ ) in common. *Trachurus* sp. was the most frequently detected fish taxon, in 84% of the samples, followed by *Scomber* sp. (66%), *Capros aper* (Linnaeus, 1758) (63%), *Ceratoscopelus maderensis* (Lowe, 1839) (50%), *Cyclothone microdon* (Günther, 1878) (42%), *Chauliodus sloani* (Bloch & Schneider, 1801) (39%) and with 32% each Zoarcidae, *Magnisudis atlantica* (Krøyer, 1868), *Lampanyctus* sp. and *Cyclopterus lumpus* (Linnaeus, 1758). The detection frequency of the other fish taxa was below 25% (Figure A2).

### 3.5 | Horizontal Distribution of Cephalopod and Fish Richness

Overall taxonomic richness tended to increase with distance from shore. The greatest cephalopod and fish richness was detected at the intermediate and offshore habitats (both  $n = 30$  for cephalopods, and  $n = 37$  and  $n = 52$  for fish, respectively), with 17 cephalopod taxa and 29 fish taxa detected inshore (Figure 3). While the intermediate and offshore habitats held more depths than the inshore habitat (i.e., 16 vs. 9 depths),

they did also hold a higher richness per depth. An average (SD) of 5 ( $\pm 3$ ) cephalopod taxa per sampling depth was detected in the inshore habitat, 7 ( $\pm 3$ ) in the intermediate habitat and 8 ( $\pm 2$ ) in the offshore habitat. The average number of fish taxa per sampling depth was 8 ( $\pm 3$ ) in the inshore habitat, 8 ( $\pm 3$ ) in the intermediate and 10 ( $\pm 3$ ) in the offshore habitat. Thus, the average number of taxa per sampling depth increased along the inshore-offshore gradient. Fish richness increased significantly across depth-binned habitats (ANOVA,  $F_{4,33} = 2.81$ ,  $p = 0.04$ ), and was highest in offshore deep habitats compared to intermediate deep habitats (Tukey's HSD,  $p = 0.03$ ) (Figure 4). However, cephalopod richness did not differ significantly in richness (ANOVA,  $F_{4,32} = 2.25$ ,  $p = 0.08$ ).

Relative read abundance of cephalopod families within the deep-scattering layer (DSL) was dominated by Enoploteuthidae and Histioteuthidae at the intermediate and offshore habitats (300–700 m). The DSL of the inshore habitat, however, was dominated by Sepiolidae, Histioteuthidae, Loliginidae, and Vampyroteuthidae (Figure 5). For fish, between 50 and 200 m, all three habitats were dominated by the families Caproidae and Carangidae, while at deeper depths, community composition became more heterogeneous, comprising a broad mix of mesopelagic and bathypelagic families.

For both taxonomic groups, the offshore habitat showed consistently higher richness across sampling depths (Figure A3), with richness changing as a function of depth, and lower overall richness in the inshore habitat as compared to offshore. Since the species accumulation curves did not reach an asymptote, additional sampling would likely uncover additional taxa. However, the rarefaction curves showed that the sequencing depth per sample was sufficient to capture the majority of diversity present within each sample, by reaching a plateau (Figures A4 and A5).

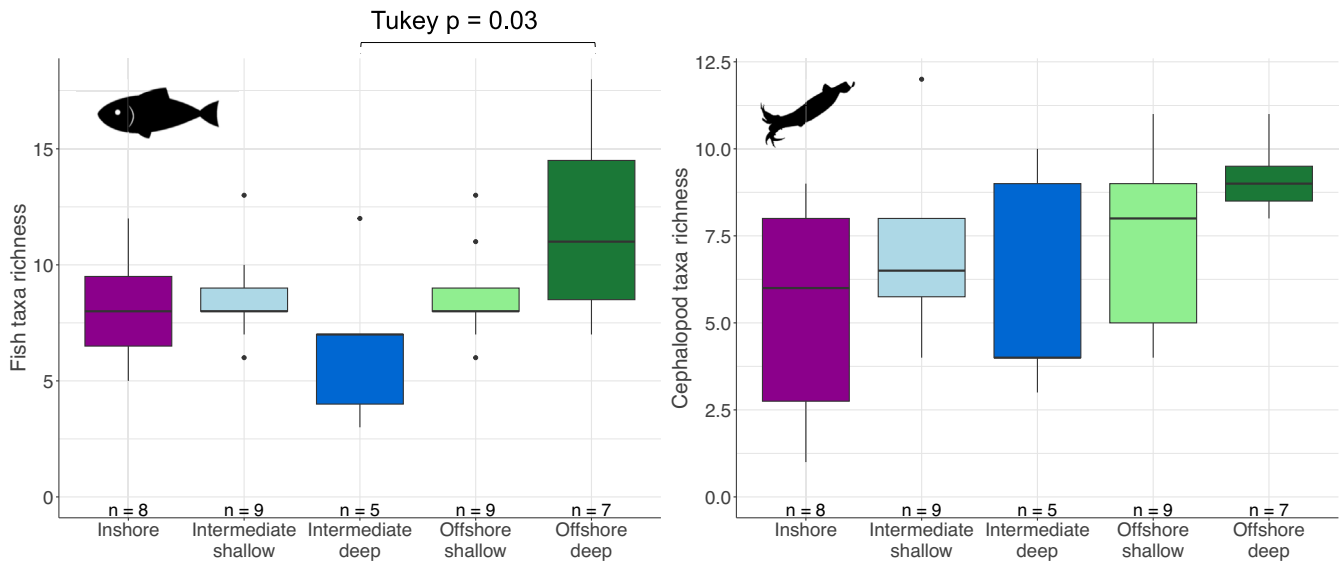


**FIGURE 4** | Fish (left) and cephalopod (right) taxonomic richness across cetacean foraging habitat zones. Sampling stations were grouped by depth for comparison: The nearshore station represented shallow waters (0–800m), while offshore stations were divided into shallow depth bins (0–800m) and deep depth bins (900m to seafloor). Inshore = Risso's dolphin (*Grampus griseus*) foraging zone, intermediate deep = Sowerby's beaked whale (*Mesoplodon bidens*) foraging zone, offshore deep = goose-beaked whale (*Ziphius cavirostris*) foraging zone. Significant pairwise differences at  $p < 0.05$ .

### 3.6 | Acoustic Backscatter Distribution With Distance From Shore

The DSL in the study area occurred between a depth of ~300–750m, along the entire inshore-offshore gradient (Figure 6). Inshore, the layer was situated deeper (max NASC at ~590–600m) than offshore (max NASC at ~460–470m), in terms of both range and depth of maximum acoustic backscatter (Figures 6 and 7). Overall acoustic backscatter significantly increased from inshore to offshore (mean sum of NASC = 3489, 6093 and 17,365  $\text{m}^2\text{nmi}^{-2}$  in inshore, intermediate and offshore habitats, respectively; GEE,  $df=2$ ,  $\chi^2=7.6$ ,  $p=0.022$ ) (Figure 6). Mean sum of NASC was 5.0 and 2.8 times higher offshore than inshore and at intermediate distances to shore, respectively, representing a significant offshore increase in total acoustic backscatter in the upper 800m (GEE; offshore vs. inshore: estimate = -13,876, SE = 5404,  $p=0.01$ ; offshore vs. intermediate: estimate = -11,272, SE = 5666,  $p=0.047$ ). The deep scattering layer bifurcated inshore (max NASC at ~590–600m and ~350m) and gradually merged into a single, continuous layer along the offshore gradient.

### 3.7 | Cephalopod and Fish Richness and Distribution With Depth and Acoustic Backscatter

Inshore, the highest cephalopod richness (8–9 taxa) was detected above the main deep scattering layer (DSL) (Figure 7A), while fish taxa richness was highest in surface waters (50–100m, 11–12 taxa) and near the seafloor at 800m (9 taxa), also outside of the main DSL (Figure 7B). The highest backscatter densities inshore were recorded in the DSL, located between 570 and 680m ( $101.6\text{--}208.3 \text{ m}^2\text{nmi}^{-2}$ , > the 75th percentile). The maximum mean ( $\pm$ SD) density,  $208.3 \text{ m}^2\text{nmi}^{-2} \pm \text{NA}$ , was recorded at a depth of 650m (Figure 7).

In the intermediate habitat, cephalopod richness also peaked above the DSL (12 taxa), and near the seafloor at 1288m (10 taxa) (Figure 7A). Fish richness followed a similar pattern, with peaks at the surface (50m, 10 taxa), intermediate depths (800m, 13 taxa), and close to the seafloor at 1288m (12 taxa) (Figure 7B). The highest backscatter densities were detected between 510 and 640m ( $111.6\text{--}182.2 \text{ m}^2\text{nmi}^{-2}$ , > the 75th percentile) and the maximum mean density was recorded at 600m ( $182.2 \pm 12.6 \text{ m}^2\text{nmi}^{-2}$ ) (Figure 7).

Offshore, cephalopod richness showed the highest values above and below the DSL at 300 and 700m (10 and 11 taxa, respectively) as well as above the bottom at 1446m (11 taxa) (Figure 7A). Fish richness was highest in surface waters (100m, 13 taxa), at intermediate depths (100m, 13 taxa) and near the seafloor at 1400 and 1446m, where it reached 18 and 16 taxa, respectively (Figure 7B). Highest backscatter densities were detected between 470 and 570m ranging between  $102.8$  and  $178.7 \text{ m}^2\text{nmi}^{-2}$  (> the 75th percentile) with the maximum recorded at 500m ( $178.7 \pm 0.1 \text{ m}^2\text{nmi}^{-2}$ ) (Figure 7).

In the bathypelagic offshore habitat (foraging depth of goose-beaked whales), cephalopod richness was relatively consistent and showed the highest values near the seafloor at 1300m and above the seafloor at 1446m (10 and 11 taxa, respectively, Figure 8A). As referred above, fish richness in the bathypelagic was highest above and near the seafloor at 1400 and 1446m, where it reached 18 and 16 taxa, respectively (Figure 8B). Highest backscatter densities were detected at 1340m in the bathypelagic ( $0.43 \pm 0.12 \text{ m}^2\text{nmi}^{-2}$ , Figure 8). Backscatter shifted deeper later in the year (June vs. August, Figure 8). While there are two peaks of backscatter at 1070–1192m and 1312–1350m in June ( $0.22 \pm 0.14\text{--}0.20 \pm 0.08$  and  $0.20 \pm 0.06\text{--}0.21 \pm 0.16 \text{ m}^2\text{nmi}^{-2}$ ), there is only one, but stronger, peak of backscatter in August between 1202 and 1352m depth ( $0.28 \pm 0.01\text{--}0.51 \pm 0.07 \text{ m}^2\text{nmi}^{-2}$ ).

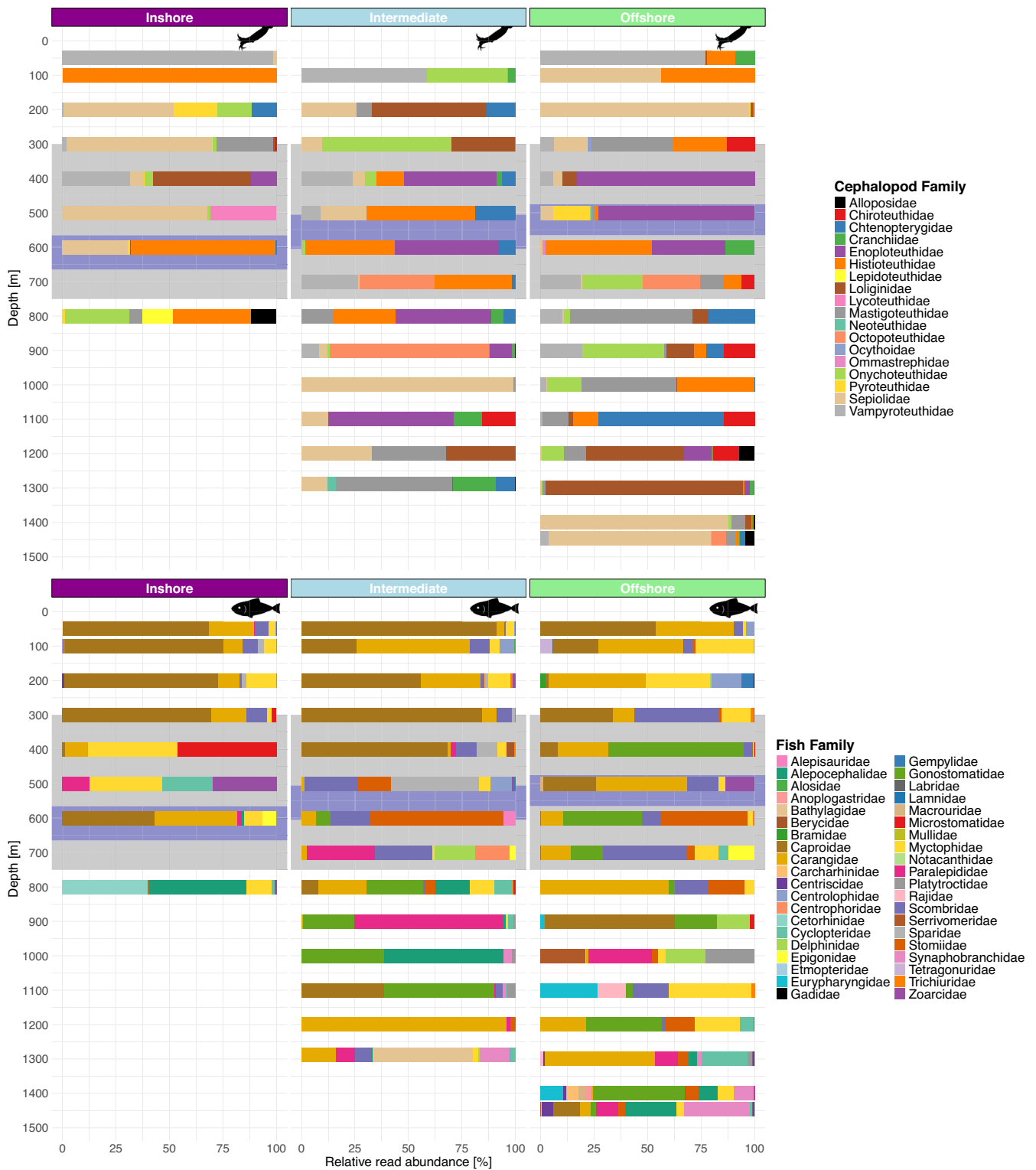


**FIGURE 5** | Cephalopod (top) and fish (bottom) family presence in the three habitats along the inshore-offshore gradient. Each horizontal bar represents the proportional contribution of read abundance for cephalopod and fish families at a given sampling depth. The light gray area depicts the location of the deep-scattering layer, and the purple shaded area the maximum acoustic backscatter detected at the specific habitats.

### 3.8 | Preyscape Characteristics in the Predator Foraging Habitats

Two significantly different fish communities were detected across the inshore-offshore gradient, differentiated as a function

of depth zone (vertical differentiation). The first community was present in surface to mesopelagic waters, including the DSL (0–800 m) and the second in lower meso- and bathypelagic waters (800–1600 m, Figure 9A, Table A4). In total, 22.6% of the variation in fish community composition could be explained by

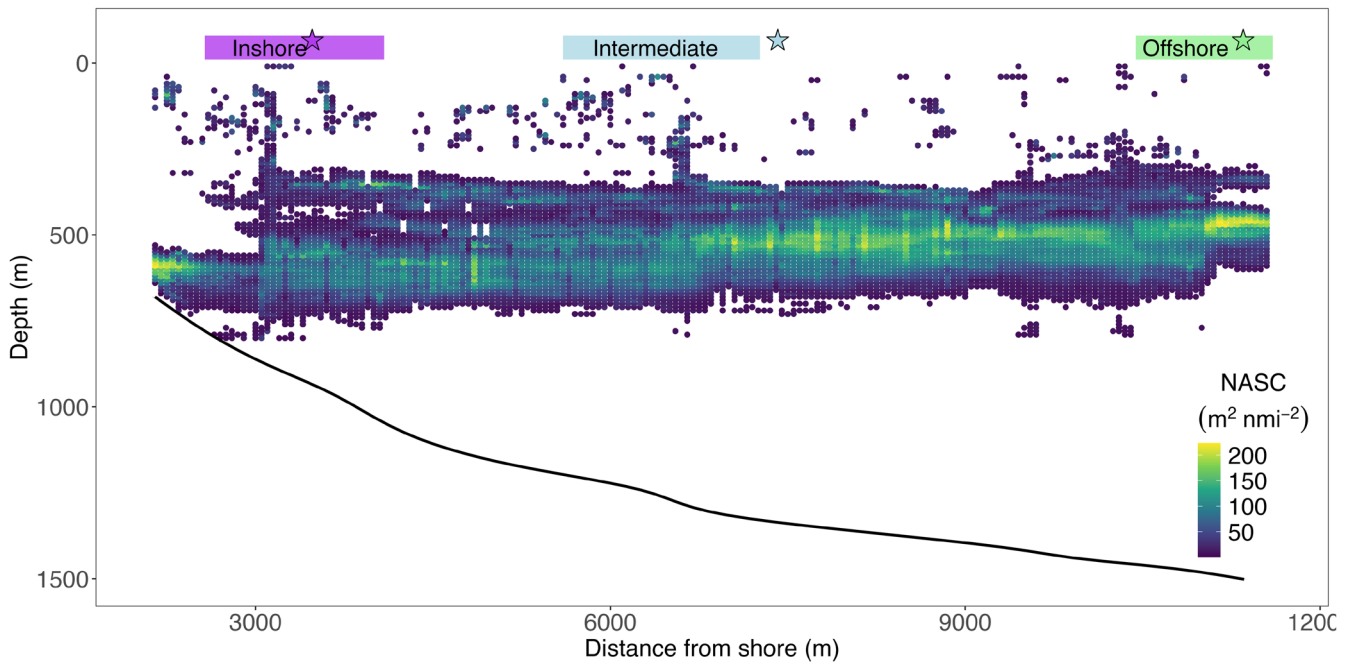


**FIGURE 6** | Inshore-offshore epi- and mesopelagic acoustic backscatter density distribution. Echogram of the nautical area scattering coefficient (NASC) as a function of depth (m) over distances from shore (m). Acoustic backscatter recording range was 5–800 m depth (surface-based echosounder). The predator core foraging habitat areas as identified in Figure 1 are indicated with colored bands, CTD locations are indicated by colored stars. Island slope bathymetry is indicated by the black solid line.

the two depth zones (PERMANOVA, 999 permutations, Jaccard,  $r^2=0.226$ ,  $p=0.001$ ). No indication was found for inshore-offshore (horizontal) differentiation.

The fish species detected by eDNA are about 10% of those known to occur in the Azores region (more than 650 species). The samples include fish taxa showing highly distinct ecologies and behavior. They comprise a few benthic, neritic taxa (i.e., Labridae, *Mullus surmuletus*, *Pagellus acarne*), abundant and commercially important bathyal, bathopelagic predatory fish (i.e., *Pagellus bogaraveo* and *Beryx* sp.), epi- to mesopelagic top predators (e.g., *Isurus oxyrinchus*, *Thunnus* sp., *Lepidocybium flavobrunneum*), a plankton feeder (*Cetorhinus maximus*), schooling epipelagic neritic species (e.g., *Trachurus* sp., *Scomber* sp., *Sardina pilchardus*, *Capros aper*, *Boops boops*), typical mesopelagic (Myctophidae spp., Stomiidae spp.) and bathypelagic taxa (*Serrivomer beanii*, *Maulisia maui*, *Sigmops bathyphilus*), and deep-sea benthic dwellers (Macrouridae, Zoarcidae, *Simenichelys parasitica*).

There is a trend linking the occurrence of neritic (and neritic-oceanic) species to the distance to shore, since the richness of those taxa was lower at the intermediate habitat that is being targeted by Sowerby's beaked whale. Conversely, the inshore habitat, targeted by Risso's dolphins, showed the lowest taxa richness of oceanic species, whether they were benthic, bathopelagic, or pelagic, along the water column. Across all three habitats, oceanic meso- to bathypelagic taxa showed the highest richness, including fish species belonging to the families Myctophidae, Stomiidae, Gonostomatidae, Paralepididae, and Platytroctidae, among other typical families and species of those midwater ecosystems (Table A3).

Cephalopod communities differed significantly between the inshore and both deep offshore habitats (pairwise.adonis,

$p_{\text{Offshore}}=0.02$  and  $p_{\text{Intermediate}}=0.045$ ) (Figure 9B, Table A5), that is between the habitats most distant from each other, indicating a potential gradual horizontal-vertical gradient in cephalopod community composition. Here, 17% of the variation was explained (PERMANOVA, 999 permutations, Jaccard,  $r^2=0.172$ ,  $p=0.002$ ).

Of the 83 known cephalopod species occurring off the Azores (Merten et al. 2021), 29% were detected with eDNA in this study. Most detected taxa were oceanic meso- to bathypelagic squid species, with two octopus taxa that are pelagic (*Haliphron atlanticus*, *Ocythoe tuberculata*). The myopsid squid, *Loligo forbesii*, is the only neritic species found in the samples and was detected in all three habitats.

#### 4 | Discussion

Using a powerful combination of hydroacoustics and eDNA, we examined surface to deep-sea nekton richness, abundance, and distribution to characterize the available deep-sea preyscapes of three coexisting toothed whale top predators. We showed that cephalopod and fish taxonomic richness varied with depth and distance from shore. Cephalopod communities showed gradual vertical and horizontal structuring between shallow depths inshore and deep depths offshore, while fish communities exhibited pronounced vertical differentiation between epi- and mesopelagic (0–800 m) and meso- to bathypelagic (900 m to the seafloor) layers. Acoustic backscatter was concentrated within the deep scattering layer (DSL). Yet, peak taxonomic richness occurred both above and below the DSL. The DSL structure also varied spatially, being deeper and bifurcated inshore, while vertically shallower and more stable offshore. Contrary to our hypothesis, the acoustic backscatter of the upper 800 m

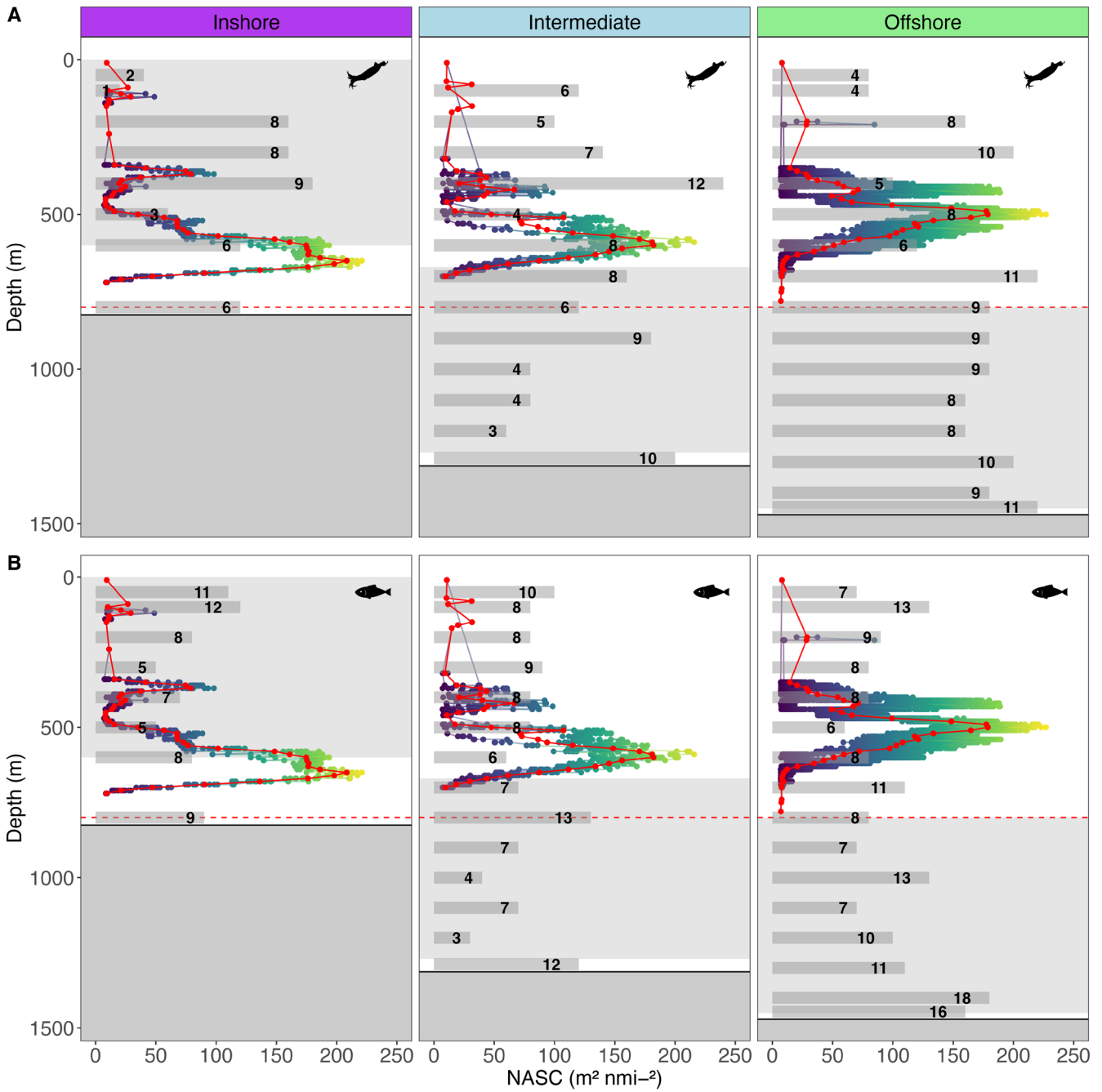


**FIGURE 7** | Cephalopod and fish taxonomic richness and acoustic density across epipelagic to bathypelagic depths. Cephalopod (A) and fish (B) taxa richness detected by eDNA overlaid with acoustic backscatter (NASC— $m^2nmi^{-2}$ , sampling range 0–800 m) across the inshore-offshore gradient. Taxa richness: Horizontal gray bars, with the number of taxa labeled within each bar. Red line: Overall mean NASC per CTD location. Red dashed line: Recording limit of hydroacoustic data. Light shaded areas represent the foraging depths of the three predators. The solid black line: The seafloor. The potential prey density at bathypelagic depths in the offshore habitat is shown in Figure 8.

was significantly higher offshore, with no decline in taxonomic richness with increasing distance from shore.

#### 4.1 | Acoustic Backscatter and Richness Along the Inshore-Offshore Gradient

Contrary to our hypothesis, density in the upper 800 m increased significantly with distance from shore. This pattern was driven by variation in the DSL acoustic backscatter at 300–700 m. This was

matched with increasing fish richness between deep intermediate and offshore habitats. Yet, cephalopod richness did not differ significantly between these habitats. The offshore DSL was shallower, more compact and had higher acoustic backscatter than the deeper and bifurcated inshore DSL. This may be caused by both physical and biological drivers. Bottom roughness (e.g., ridges or seamounts) and coastal upwelling can enhance ocean mixing and may alter the stability and vertical distribution of the DSL closer to shore (Kunze and Llewellyn Smith 2004). Similarly, coastal upwelling has been associated with DSL disruption and reduced

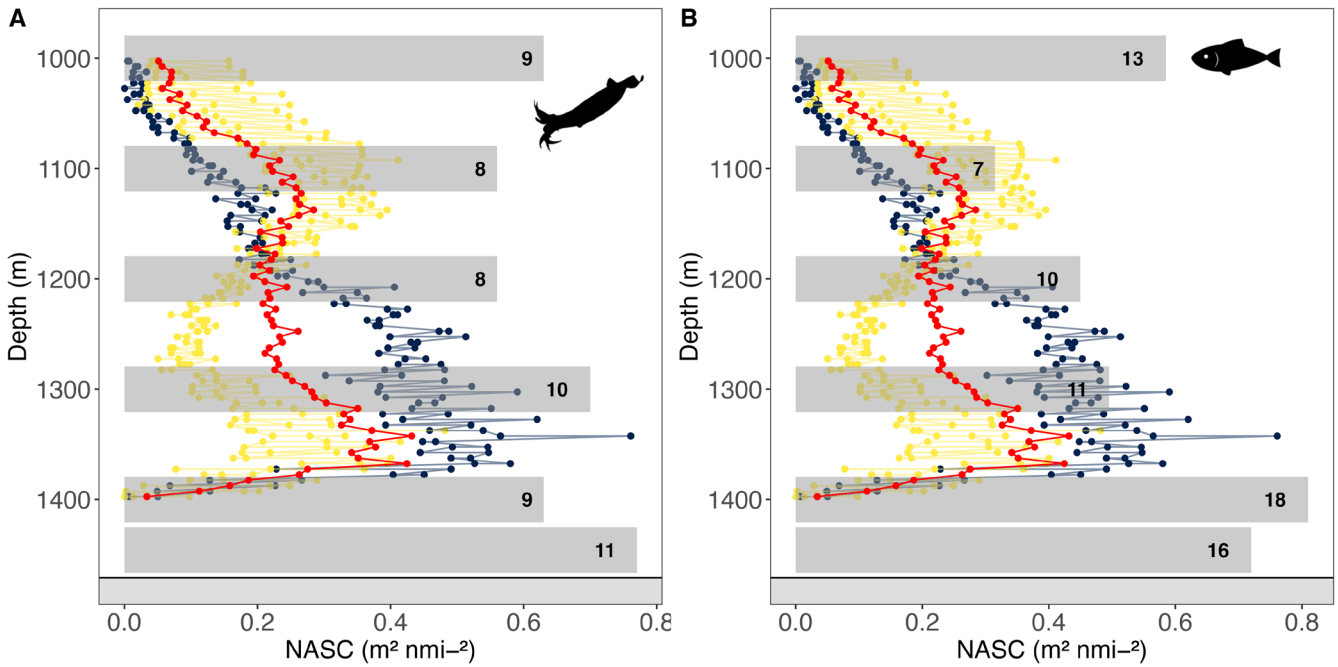


**FIGURE 8** | Bathypelagic taxa richness and potential prey density in the offshore habitat. Cephalopod (A) and fish (B) taxonomic richness from eDNA metabarcoding overlaid with the nautical area scattering coefficient (NASC;  $S_A$ — $m^2nmi^{-2}$ ) derived from a moored 70 kHz echosounder (WBAT; range 1400–1000 m). Horizontal gray bars: taxa richness, with the numbers of detected taxa labeled within each bar. Red line: overall mean  $S_A$  across sampling time periods. Black line: seafloor. Yellow lines: June  $S_A$  values. Dark blue lines: August  $S_A$  values.

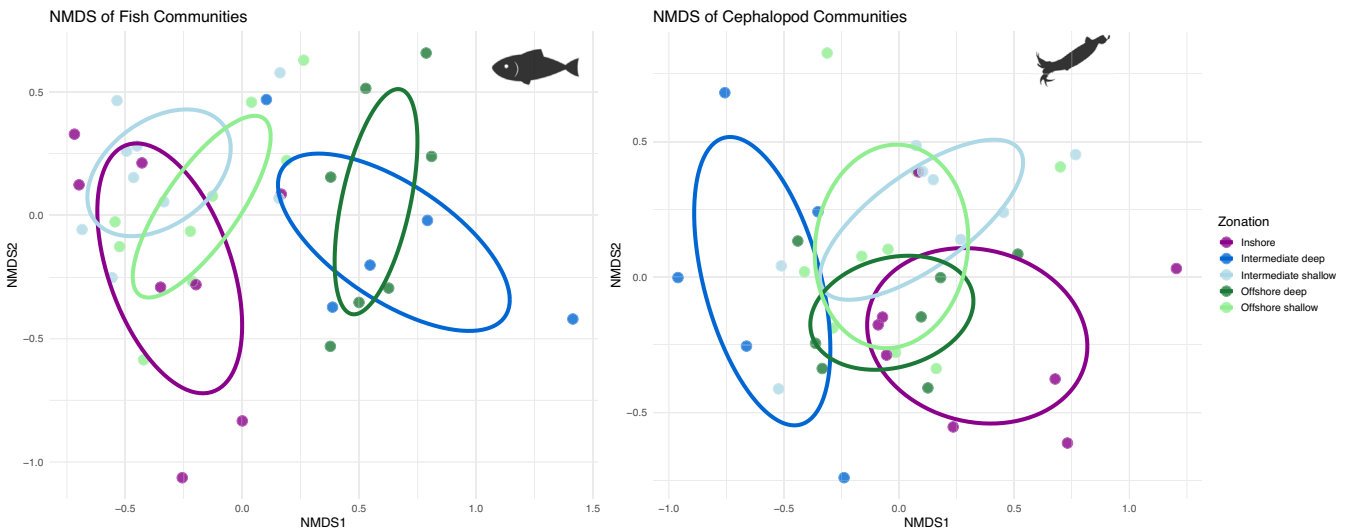


**FIGURE 9** | Horizontal and vertical differentiation in fish and cephalopod community composition across the inshore-offshore gradient. Non-metric multidimensional scaling (NMDS) plots illustrate community composition based on presence/absence data (Jaccard Index) for fish (left) and cephalopods (right), derived from eDNA metabarcoding. Stress value indicates good ordination fit (fish: 0.1533; cephalopods: 0.1693). “Inshore” is the foraging depth of Risso’s dolphins. “Intermediate deep” the foraging depths of Sowerby’s beaked whales and “offshore deep” the foraging depths of goose-beaked whales.

acoustic backscatter (Diogoul et al. 2020). Additionally, oxygen concentration and availability may play a role. The inshore oxygen profile remains stable to ~600 m before declining, whereas offshore oxygen decreases from ~350 m, potentially influencing vertical prey distribution and aggregation patterns (Hoving et al. 2020).

Predator avoidance behavior of mesopelagic organisms could be one of the biological drivers of the distribution of the DSL inshore, that is, the DSL may respond to foraging odontocetes by moving

deeper (Benoit-Bird et al. 2017; Urmey and Benoit-Bird 2021). The predation pressure by bathypelagic fish dwelling on the island slope (and seamounts) and relying on autochthonous food sources such as advected midwater fish and cephalopods (Sutton et al. 2007) might further explain the lower inshore acoustic backscatter. Large migratory schooling fish predators (e.g., tuna) are also known to feed close to island shores and increase the predation pressure on prey taxa. In the Gulf of Corinth, the DSL bifurcates into a shallow non-migrant thin layer at 150 to 280 m and

a deeper, thick, partially migratory layer between 250 and 600 m (Kapelonis et al. 2023). Since the sampling here was restricted to daytime surveys, we cannot assess diel vertical migration patterns directly. Yet, the structure we observe may reflect a similar layering, potentially shaped by non-migrant and migratory organisms. Together, these oceanographic gradients suggest that both biological and physical processes shape the structure and detectability of prey layers across the inshore-offshore axis.

#### 4.2 | Acoustic Backscatter and Taxonomic Richness From Surface to Bottom

Deep-sea acoustic backscatter density and richness were inversely related. Whereas the bulk of the acoustic backscatter in the top 800 m resided in the DSL, the highest taxa richness was systematically detected above or below this layer. This is surprising and suggests that DSL internal richness of fishes and cephalopods may be relatively low. Most fish taxa detected with eDNA were benthic, bathypelagic, or epipelagic species, which are not known to be part of the DSL. Yet, the detected myctophid fishes are usually primarily found in the DSL (Barham 1966). Alternatively, much of the acoustic backscatter in the DSL may originate from fauna other than cephalopods or fishes, such as gelatinous zooplankton (e.g., physonect siphonophores) (Barham 1966; Proud et al. 2019). Acoustic and net-sampling studies have shown that the DSL signal is often dominated by a few scattering species or many non-fish scatterers, reducing apparent internal richness (Benoit-Bird et al. 2017; Sato and Benoit-Bird 2017).

Community structuring exhibited an opposite pattern at bathypelagic depths, where richness increased in parallel with acoustic backscatter. However, acoustic backscatter was structurally much lower. This was particularly true for the benthic boundary layer, that is, the water mass that extends to ~100 m above the seafloor (Angel 1990; Robison 2004). The localized buildup of acoustic backscatter in the bathypelagic may reflect a structurally and functionally diverse community, potentially driven by benthic-pelagic coupling, higher trophic complexity, or fine-scale habitat heterogeneity near the seafloor. Additionally, the extended vertical distribution of many pelagic species allows for their interaction with the bottom, compressing species toward the benthic-boundary layer that would otherwise be dispersed in the water column, resulting in an increase in taxonomic richness and acoustic backscatter.

#### 4.3 | Fish and Cephalopod Community Structure Differentiate Across Horizontal and Vertical Gradients

Cephalopod and fish communities exhibited contrasting spatial patterns. Fish assemblages were structured primarily by depth and showed uniformity with distance from shore, whereas cephalopods displayed more gradual differentiation with increasing depth and distance from shore. The broad vertical distribution of cephalopod eDNA likely reflects their typically broad vertical distribution ranges and, across their life cycle, the capacity of some cephalopods to swim thousands of meters daily as part of diel vertical movement, predator avoidance, and foraging strategies (Hoving et al. 2014; Judkins

and Vecchione 2020; Roper and Young 1975). In contrast, fish eDNA exhibited clear vertical zonation across all habitats, with shallow-water communities (50–800 m) differing significantly from those found at greater depths (>800 to the seafloor). Distinct cephalopod assemblages observed between inshore and deep offshore habitats differed from previous findings in the same area (Visser, Merten, et al. 2021), potentially reflecting interannual shifts in cephalopod abundance and food availability or environmental conditions that may have a pronounced influence on cephalopod recruitment and growth (Rodhouse et al. 2014).

Several of the detected fish taxa represent first records for the Azores. The most surprising was the detection of eDNA from lumpfish *Cyclopterus lumpus* across all habitats. This species normally lives between 50 and 150 m over rocky bottom in cold-temperate subpolar waters. Juvenile lumpfish are known to associate and disperse with floating seaweed, such as *Sargassum* (Ingólfsson and Kristjánsson 2002; Vandendriessche et al. 2007). The Azores, situated along major transatlantic maritime routes, frequently receive floating seaweed, which facilitates the arrival of non-native species (Gabriel, Martins, et al. 2024). In 2024, a large-scale *Sargassum* inundation was reported for the first time along the Azorean coast, potentially introducing species such as lumpfish (Gabriel, Maridakis, et al. 2024).

The eDNA detections of the three fish species *Diplospinus multistriatus*, *Notacanthus chemnitzii*, and *Nansenia boreacrassicauda* represent the first records of these taxa in Azorean waters (Froese and Pauly 2000; Santos et al. 1997). It is plausible that these species may occur in the region but have previously gone undetected due to limited deep-sea sampling effort and the cryptic nature of many bathypelagic species. This highlights the power of eDNA metabarcoding to uncover hidden biodiversity and expand our understanding of species distributions.

#### 4.4 | Predator Preyscape Differentiation

Preyscapes across habitats varied in acoustic backscatter and partly in taxonomic richness, and prey communities. Risso's dolphins hunt inshore predominantly on cephalopods in 200–600 m depth at the upper (daytime) or lower (night time) margin of the DSL (Visser, Keller, et al. 2021). This foraging habitat was characterized by lower overall acoustic backscatter and a trend toward reduced richness, as compared to more offshore habitats. Yet, with the presence of the DSL, density is much higher than in the deeper foraging zones targeted by, for example, goose-beaked whales. Risso's dolphins foraging habitats are accessible to a range of other cetaceans and marine predators, potentially creating a more competitive foraging environment. However, Risso's dolphins typically occur in larger groups and form long-term social associations, which may be advantageous in competitive or predator-rich settings (Hartman et al. 2008; Shane 1995). In contrast, goose-beaked whales usually forage in small groups and are thought to have limited capacity for active competition or defense (Aguilar de Soto et al. 2020).

It may be that goose-beaked whales forage in the bathypelagic to target larger, more mature prey that occur in deeper

waters as a result of ontogenetic migration (Visser, Merten, et al. 2021). However, until now, direct data on potential prey acoustic backscatter and density within goose-beaked whale foraging zones were limited. Here, hydroacoustic data from depths between 1000 and 1446 m in the offshore habitat revealed sparse prey aggregations, while eDNA analyses indicated high taxonomic richness. This strengthens the hypothesis that goose-beaked whales may target dispersed but taxonomically diverse prey rather than dense, homogeneous shoals. Off southern California, goose-beaked whales forage in areas characterized by lower densities of myctophids, squid, and other micronekton than areas they use less frequently for foraging. Despite reduced standing stocks across multiple trophic levels, goose-beaked whales could still forage (Benoit-Bird et al. 2016). These findings imply that prey quality, behavior, or spatial configuration may outweigh bulk abundance for these predators. Unlike the California system, prey acoustic backscatter in the goose-beaked whale's habitat in our study varied with depth, potentially reflecting regional differences in preyscape structure or oceanography. Off Terceira, goose-beaked whale foraging habitats align with slopes of submarine canyons that trap organic matter and support benthic productivity (De Leo et al. 2010; Fernandez-Arcaya et al. 2017; Pearman et al. 2023). Yet, these habitats likely support lower densities of larger prey compared to the mesopelagic, where smaller but more abundant individuals are present (Hoving et al. 2014). Consequently, goose-beaked whales may adopt deep offshore foraging strategies to target larger, high-quality prey despite lower encounter rates. Despite their size, they make fewer foraging dives and capture attempts than Risso's dolphins (Visser, Merten, et al. 2021), supporting the idea that they prioritize prey quality over encounter rate.

Sowerby's beaked whales are the only species of the three cetaceans investigated here to predominantly feed on fish and just occasionally on cephalopods (MacLeod et al. 2003; Pereira et al. 2011; Spitz et al. 2011). Their foraging habitat is at intermediate distances to shore, but overlaps with the goose-beaked whales' offshore foraging habitat. Their preyscape shows similar fish richness compared to inshore habitats, yet reduced fish richness compared to the deep offshore habitat. According to diet studies based on stranded individuals, Sowerby's beaked whales in the Azores predominantly feed on numerically abundant midwater prey such as Myctophidae, Melamphidae, and Diretmidae with Myctophidae being the main component of the DSL (Pereira et al. 2011). Bottom-dwelling fish like gadids and merlucciids, characteristic of Sowerby's beaked whale diet in other regions (MacLeod et al. 2003; Spitz et al. 2011), appear to be rare prey in Azorean waters. Net sampling (Pereira et al. 2011) and our eDNA data detected only a single gadid species and no merlucciids.

Sowerby's and goose-beaked whales maintain relatively high prey capture rates (e.g., 17–42 prey capture attempts per dive and 30–34 prey capture attempts per hour, respectively) (Visser et al. 2022; Visser, Merten, et al. 2021), indicating effective foraging even in low-density environments. Risso's dolphins have the potency to extract more energy per hour of foraging compared to goose-beaked whales (Guilpin et al. 2025), suggesting that nearshore habitats, though potentially less diverse, may offer higher energetic returns. This highlights that predator

success is not solely determined by prey density, but also by prey accessibility, spatial distribution and energetic payoff (Benoit-Bird et al. 2013). Such dynamics likely underpin the fine-scale habitat separation at the km<sup>2</sup>-scale observed among these deep-diving cetaceans.

Although the deep-diving cetaceans observed in the study area do not directly target the offshore DSL (deep layer at 300–750 m), aside from Sowerby's beaked (Pereira et al. 2011), the DSL likely sustains intermediate predators such as cephalopods and fish, which hunt and capitalize on its abundant resources, but do not reside permanently within the DSL. Indeed, eDNA from some of those intermediate predators, such as ommastrephid squids, sharks and bony fish (e.g., trichiurids, gempylids, scombrids) was detected in the sampling area. Foraging just above and occasionally in the DSL has also been observed for large squids such as *Loligo forbesi* and *Dosidicus gigas* (Cones et al. 2022; Gilly et al. 2006). In turn, beaked whales may consume these foraging cephalopods and fish that occur in small groups or as solitary individuals in deeper layers. Previous research has found that beaked whales tended to increase foraging effort where there were larger single prey items below the DSL (Hazen et al. 2011) and that predator density was related to DSL density and composition as well (Hazen and Johnston 2010). Thus, while some deep-diving cetaceans may not exploit the DSL directly, the DSL may play an important role in structuring the prey field upon which these whales depend.

Additionally, cetaceans are not the only deep-hunting predators. Sharks represent another group potentially competing with cetaceans for cephalopod and fish prey. Our eDNA data detected six shark species co-occurring in the habitats of the cetacean species, including lantern sharks (*Etmopterus* sp.), blue sharks (*Prionace glauca*), and shortfin mako sharks (*Isurus oxyrinchus*), all known consumers of mesopelagic and bathypelagic prey (Jakobsdóttir 2001; Nakano and Stevens 2008; Stevens 2008). These detections highlight the ecological overlap among deep-diving predators with varied physiological specificities and underscore the need to consider multispecies interactions when evaluating trophic dynamics and conservation priorities in oceanic ecosystems.

## 5 | Conclusion

Our findings highlight the importance of vertical and horizontal habitat complexity in supporting predator–prey interactions and cetacean habitat partitioning. Long-term monitoring of preyscape dynamics at seasonal and interannual scales is vital for understanding ecosystem variability. While net sampling has traditionally been used to assess prey distribution, it offers limited spatial resolution and can underestimate mobile prey (Kaartvedt et al. 2012; Kimura and Somerton 2006). In contrast, integrating eDNA, hydroacoustics, and biologging provides high spatial and temporal resolution to detect changes in prey community structure and acoustic backscatter. Future research should incorporate multi-frequency acoustics to resolve prey type and density, directly link predator behavior to preyscape characteristics through predator and prey tagging, and conduct in situ observations to document predator–prey interactions.

## Author Contributions

F.V. and H.-J.H. conceived the study. F.V., H.-J.H., V.M., and M.G. designed the study. F.V., M.G., M.O., S.M.D., S.B.-P. collected the hydroacoustic data. V.M., J.M.P., and M.F.G. conducted the sampling and laboratory analysis; M.G. and S.M.D. conducted the analysis of hydroacoustic data. V.M., J.M.P., M.G., S.M.D., and M.O. performed formal analysis and processing. Writing – original draft: V.M. and M.G. Writing – review and editing: All authors. T.B. provided critical support during eDNA analysis and interpretation. S.F. performed the sequencing. All authors critically revised the manuscript. All authors gave final approval for publication and agreed to be held accountable for the work performed therein.

## Acknowledgments

This project was funded by the Office of Naval Research Marine Mammal Biology Program, USA (ONR; grant numbers N00014-20-1-2702 and N00014-22-1-2605; program manager, M. Weise), the Dutch Research Council (NWO; Veni grant 016. Veni.181.086), the German Research Foundation [DFG; Emmy Noether Independent Junior Research Group grant of H.J.T. Hoving (HO 5569/2-1)], and Helmholtz POF III and POF IV program. We thank all members of the field team for their dedication and support throughout the project. We are also grateful to the captain and crew of the RV *Pelagia* for their excellent collaboration and assistance during the research cruise. Open Access funding enabled and organized by Projekt DEAL.

## Funding

This work was supported by the Office of Naval Research Marine Mammal Biology Program, USA (Grants N00014-20-1-2702 and N00014-22-1-2605), NWO; Veni Grant 016 (Grant Veni.181.086), FG; Emmy Noether Independent Junior Research Group (Grant HO 5569/2-1), and Helmholtz POF III and POF IV.

## Ethics Statement

Fieldwork was conducted under scientific permits issued by the Direção Regional dos Assuntos do Mar, Secretaria Regional do Mar, Ciência e Tecnologia (Regional Directorate for Science and Technology). Access and Benefit Sharing (ABS) Regulation: Portugal is party to the Nagoya Protocol but does not regulate access to genetic resources. The ABS regulations of the Autonomous Region of the Azores were followed by obtaining the required declaration of conformity, establishing informed consent for the collection and export of biological material from the Direção Regional da Ciência e Tecnologia. The manuscript has not been submitted elsewhere.

## Conflicts of Interest

The authors declare no conflicts of interest.

## Data Availability Statement

The data that support the findings of this study are openly available in Genbank Sequence Read Archive at [www.ncbi.nlm.nih.gov/genbank](http://www.ncbi.nlm.nih.gov/genbank), reference numbers SUB15426879, (18S Cephalopod) and PRJNA1295789 (16S Cephalopod). The fish sequencing data are available upon request. Additional metadata for the raw sequences are found in the [Supporting Information](#). Any enquiries should be directed to the corresponding author. The hydroacoustic data supporting the findings of this study are available in the NIOZ DAS database (contact F. Visser).

## References

Afonso, P., J. Fontes, E. Giacomello, et al. 2020. “The Azores: A Mid-Atlantic Hotspot for Marine Megafauna Research and Conservation.”

*Frontiers in Marine Science* 6: 826. <https://doi.org/10.3389/fmars.2019.00826>.

Aguilar de Soto, N., F. Visser, P. L. Tyack, et al. 2020. “Fear of Killer Whales Drives Extreme Synchrony in Deep Diving Beaked Whales.” *Scientific Reports* 10: 13. <https://doi.org/10.1038/s41598-019-55911-3>.

Angel, M. V. 1990. “Life in the Benthic Boundary Layer: Connections to the Mid-Water and Sea Floor.” *Philosophical Transactions of the Royal Society of London. Series A, Mathematical and Physical Sciences* 331: 15–28. <https://doi.org/10.1098/rsta.1990.0053>.

Arce, F., M. A. Hindell, C. R. McMahon, et al. 2022. “Elephant Seal Foraging Success Is Enhanced in Antarctic Coastal Polynyas.” *Proceedings of the Royal Society B: Biological Sciences* 289: 20212452. <https://doi.org/10.1098/rspb.2021.2452>.

Arostegui, M. C., P. Gaube, M. L. Berumen, et al. 2020. “Vertical Movements of a Pelagic Thresher Shark (*Alopias pelagicus*): Insights Into the Species’ Physiological Limitations and Trophic Ecology in the Red Sea.” *Endangered Species Research* 43: 387–394.

Bailleul, F., J.-B. Charrassin, P. Monestiez, F. Roquet, M. Biuw, and C. Guinet. 2007. “Successful Foraging Zones of Southern Elephant Seals From the Kerguelen Islands in Relation to Oceanographic Conditions.” *Philosophical Transactions of the Royal Society, B: Biological Sciences* 362: 2169–2181. <https://doi.org/10.1098/rstb.2007.2109>.

Barham, E. G. 1966. “Deep Scattering Layer Migration and Composition: Observations From a Diving Saucer.” *Science* 151: 1399–1403. <https://doi.org/10.1126/science.151.3716.1399>.

Barlow, J., M. Kahru, and B. G. Mitchell. 2008. “Cetacean Biomass, Prey Consumption, and Primary Production Requirements in the California Current Ecosystem.” *Marine Ecology Progress Series* 371: 285–295.

Barton, E. D., G. Basterretxea, P. Flament, et al. 2000. “Lee Region of Gran Canaria.” *Journal of Geophysical Research: Oceans* 105: 17173–17193. <https://doi.org/10.1029/2000JC900010>.

Benoit-Bird, K. J., B. C. Battaile, S. A. Heppell, et al. 2013. “Prey Patch Patterns Predict Habitat Use by Top Marine Predators With Diverse Foraging Strategies.” *PLoS One* 8: e53348. <https://doi.org/10.1371/journal.pone.0053348>.

Benoit-Bird, K. J., and G. L. Lawson. 2016. “Ecological Insights From Pelagic Habitats Acquired Using Active Acoustic Techniques.” *Annual Review of Marine Science* 8: 463–490. <https://doi.org/10.1146/annurev-marine-122414-034001>.

Benoit-Bird, K. J., M. A. Moline, and B. L. Southall. 2017. “Prey in Oceanic Sound Scattering Layers Organize to Get a Little Help From Their Friends.” *Limnology and Oceanography* 62: 2788–2798. <https://doi.org/10.1002/lno.10606>.

Benoit-Bird, K. J., B. L. Southall, and M. A. Moline. 2016. “Predator-Guided Sampling Reveals Biotic Structure in the Bathypelagic.” *Proceedings of the Royal Society B: Biological Sciences* 283: 20152457. <https://doi.org/10.1098/rspb.2015.2457>.

Berger, C. S., B. Bougas, S. Turgeon, S. Ferchiou, N. Ménard, and L. Bernatchez. 2020. “Groundtruthing of Pelagic Forage Fish Detected by Hydroacoustics in a Whale Feeding Area Using Environmental DNA.” *Environmental DNA* 2: 477–492. <https://doi.org/10.1002/edn3.73>.

Braun, C. D., M. C. Arostegui, S. R. Thorrold, et al. 2022. “The Functional and Ecological Significance of Deep Diving by Large Marine Predators.” *Annual Review of Marine Science* 14: 129–159. <https://doi.org/10.1146/annurev-marine-032521-103517>.

Braun, C. D., A. Della Penna, M. C. Arostegui, et al. 2023. “Linking Vertical Movements of Large Pelagic Predators With Distribution Patterns of Biomass in the Open Ocean.” *Proceedings of the National Academy of Sciences of the United States of America* 120: e2306357120. <https://doi.org/10.1073/pnas.2306357120>.

- Braun, C. D., P. Gaube, P. Afonso, J. Fontes, G. B. Skomal, and S. R. Thorrold. 2019. "Assimilating Electronic Tagging, Oceanographic Modelling, and Fisheries Data to Estimate Movements and Connectivity of Swordfish in the North Atlantic." *ICES Journal of Marine Science* 76: 2305–2317. <https://doi.org/10.1093/icesjms/fsz106>.
- Braun, C. D., N. Lezama-Ochoa, N. Farchadi, et al. 2023. "Widespread Habitat Loss and Redistribution of Marine Top Predators in a Changing Ocean." *Science Advances* 9: eadi2718. <https://doi.org/10.1126/sciadv.adi2718>.
- Cade, D. E., and K. J. Benoit-Bird. 2014. "An Automatic and Quantitative Approach to the Detection and Tracking of Acoustic Scattering Layers." *Limnology and Oceanography: Methods* 12: 742–756. <https://doi.org/10.4319/lom.2014.12.742>.
- Caldeira, R. M. A., S. Groom, P. Miller, D. Pilgrim, and N. P. Nezlin. 2002. "Sea-Surface Signatures of the Island Mass Effect Phenomena Around Madeira Island, Northeast Atlantic." *Remote Sensing of Environment* 80: 336–360. [https://doi.org/10.1016/S0034-4257\(01\)00316-9](https://doi.org/10.1016/S0034-4257(01)00316-9).
- Callahan, B. J., P. J. McMurdie, M. J. Rosen, A. W. Han, A. J. A. Johnson, and S. P. Holmes. 2016. "DADA2: High-Resolution Sample Inference From Illumina Amplicon Data." *Nature Methods* 13: 581–583. <https://doi.org/10.1038/nmeth.3869>.
- Campanella, F., M. A. Collins, E. F. Young, V. Laptikhovskiy, P. Whomersley, and J. van der Kooij. 2021. "First Insight of Meso- and Benthic-Pelagic Fish Dynamics Around Remote Seamounts in the South Atlantic Ocean." *Frontiers in Marine Science* 8: 663278. <https://doi.org/10.3389/fmars.2021.663278>.
- Clarke, M. R. 1977. "Beaks, Nets and Numbers." *Symposia of the Zoological Society of London* 38: 89–126.
- Clarke, M. R. 1996. "Cephalopods as Prey. III. Cetaceans." *Philosophical Transactions of the Royal Society, B: Biological Sciences* 351: 1053–1065. <https://doi.org/10.1098/rstb.1996.0093>.
- Cones, S. F., D. Zhang, A. K. Shorter, et al. 2022. "Swimming Behaviors During Diel Vertical Migration in Veined Squid *Loligo forbesii*." *Marine Ecology Progress Series* 691: 83–96.
- de Jonge, D., V. Merten, T. Bayer, O. Puebla, T. B. H. Reusch, and H.-J. T. Hoving. 2021. "A Novel Metabarcoding Primer Pair for Environmental DNA Analysis of Cephalopoda (Mollusca) Targeting the Nuclear 18S rRNA Region." *Royal Society Open Science* 8: rsos.201388. <https://doi.org/10.1098/rsos.201388>.
- De Leo, F. C., C. R. Smith, A. A. Rowden, D. A. Bowden, and M. R. Clark. 2010. "Submarine Canyons: Hotspots of Benthic Biomass and Productivity in the Deep Sea." *Proceedings of the Royal Society B: Biological Sciences* 277: 2783–2792. <https://doi.org/10.1098/rspb.2010.0462>.
- De Robertis, A., and I. Higginbottom. 2007. "A Post-Processing Technique to Estimate the Signal-To-Noise Ratio and Remove Echosounder Background Noise." *ICES Journal of Marine Science* 64: 1282–1291. <https://doi.org/10.1093/icesjms/fsm112>.
- Demer, D. A., L. Berger, M. Bernasconi, et al. 2015. *Calibration of Acoustic Instruments*. ICES Cooperative Research Report No. 326, 133. <https://doi.org/10.17895/ices.pub.5494>.
- Diogoul, N., P. Brehmer, Y. Perrot, et al. 2020. "Fine-Scale Vertical Structure of Sound-Scattering Layers Over an East Border Upwelling System and Its Relationship to Pelagic Habitat Characteristics." *Ocean Science* 16: 65–81. <https://doi.org/10.5194/os-16-65-2020>.
- Easson, C. G., K. M. Boswell, N. Tucker, J. D. Warren, and J. V. Lopez. 2020. "Combined eDNA and Acoustic Analysis Reflects Diel Vertical Migration of Mixed Consortia in the Gulf of Mexico." *Frontiers in Marine Science* 7: 552. <https://doi.org/10.3389/fmars.2020.00552>.
- Fernandez-Arcaya, U., E. Ramirez-Llodra, J. Aguzzi, et al. 2017. "Ecological Role of Submarine Canyons and Need for Canyon Conservation: A Review." *Frontiers in Marine Science* 4: 5. <https://doi.org/10.3389/fmars.2017.00005>.
- Foote, K. G., H. P. Knudsen, G. Vestnes, D. N. MacLennan, and E. J. Simmonds. 1987. *Calibration of Acoustic Instruments for Fish Density Estimation: A Practical Guide*. ICES Cooperative Research Reports (CRR). Report. <https://doi.org/10.17895/ices.pub.8265>.
- Fox, J., and S. Weisberg. 2019. *Car: An R Companion to Applied Regression*. 3rd ed. R Package Version 3.1-3. <https://cran.r-project.org/web/packages/car>.
- Friedlaender, A. S., G. L. Lawson, and P. N. Halpin. 2009. "Evidence of Resource Partitioning Between Humpback and Minke Whales Around the Western Antarctic Peninsula." *Marine Mammal Science* 25: 402–415.
- Froese, R., and D. Pauly. 2000. *FishBase. World Wide Web Electronic Publication* [WWW Document]. Accessed July 22, 2022. [www.fishbase.org](http://www.fishbase.org).
- Gabriel, D., C. Maridakis, and S. Fredericq. 2024. "Gone With the Wind: An Unexpected *Sargassum inundation* in the Mid-Atlantic Azores Archipelago." *Marine Pollution Bulletin* 204: 116522. <https://doi.org/10.1016/j.marpolbul.2024.116522>.
- Gabriel, D., B. Martins, C. Ribeiro, et al. 2024. "Quantification of the Invasiveness Risk of Non-Native Macroalgae in the Azores to Support Conservation Measures." *Aquatic Conservation: Marine and Freshwater Ecosystems* 34: e4082. <https://doi.org/10.1002/aqc.4082>.
- Gilly, W. F., U. Markaida, C. H. Baxter, et al. 2006. "Vertical and Horizontal Migrations by the Jumbo Squid *Dosidicus gigas* Revealed by Electronic Tagging." *Marine Ecology Progress Series* 324: 1–17.
- Goldbogen, J. A., E. L. Hazen, A. S. Friedlaender, et al. 2015. "Prey Density and Distribution Drive the Three-Dimensional Foraging Strategies of the Largest Filter Feeder." *Functional Ecology* 29: 951–961. <https://doi.org/10.1111/1365-2435.12395>.
- Gove, J. M., M. A. McManus, A. B. Neuheimer, et al. 2016. "Near-Island Biological Hotspots in Barren Ocean Basins." *Nature Communications* 7: 10581. <https://doi.org/10.1038/ncomms10581>.
- Grassian, B., C. Roman, J. D. Warren, and D. Casagrande. 2023. "High-Resolution Measurements of the Epipelagic and Mesopelagic Ocean by a Profiling Vehicle Equipped With Environmental Sensors and a Broadband Echosounder." *Limnology and Oceanography: Methods* 21: 106–125. <https://doi.org/10.1002/lom3.10532>.
- Guilpin, M., E. Bronswijk, M. Sadde, et al. 2025. "Calories of the Deep: Energy-Rich Cephalopods Fuel Oceanic Top Predators." *Nature Ecology & Evolution in Review*.
- Hardin, J. W., and J. M. Hilbe. 2002. *Generalized Estimating Equations*. 2nd ed. Chapman and Hall/CRC.
- Haris, K., R. J. Kloser, T. E. Ryan, and J. Malan. 2018. "Deep-Water Calibration of Echosounders Used for Biomass Surveys and Species Identification." *ICES Journal of Marine Science* 75: 1117–1130. <https://doi.org/10.1093/icesjms/fsx206>.
- Hartman, K. L., F. Visser, and A. J. E. Hendriks. 2008. "Social Structure of Risso's Dolphins (*Grampus griseus*) at the Azores: A Stratified Community Based on Highly Associated Social Units." *Canadian Journal of Zoology* 86: 294–306. <https://doi.org/10.1139/Z07-138>.
- Hazen, E. L., and D. W. Johnston. 2010. "Meridional Patterns in the Deep Scattering Layers and Top Predator Distribution in the Central Equatorial Pacific." *Fisheries Oceanography* 19: 427–433. <https://doi.org/10.1111/j.1365-2419.2010.00561.x>.
- Hazen, E. L., S. Jorgensen, R. R. Rykaczewski, et al. 2013. "Predicted Habitat Shifts of Pacific Top Predators in a Changing Climate." *Nature Climate Change* 3: 234–238. <https://doi.org/10.1038/nclim.ate1686>.
- Hazen, E. L., D. P. Nowacek, L. St. Laurent, P. N. Halpin, and D. J. Moretti. 2011. "The Relationship Among Oceanography, Prey Fields, and Beaked Whale Foraging Habitat in the Tongue of the Ocean." *PLoS One* 6: e19269. <https://doi.org/10.1371/journal.pone.0019269>.

- Hazen, E. L., R. M. Suryan, J. A. Santora, S. J. Bigrad, Y. Watanuki, and R. P. Wilson. 2013. "Scales and Mechanisms of Marine Hotspot Formation." *Marine Ecology Progress Series* 487: 177–183.
- Herring, P. 2002. *The Biology of the Deep Ocean*. Oxford University Press.
- Højsgaard, S., U. Halekoh, and J. Yan. 2005. "The R Package Geepack for Generalized Estimating Equations." *Journal of Statistical Software* 15: 1–11. <https://doi.org/10.18637/jss.v015.i02>.
- Houghton, J. D. R., T. K. Doyle, J. Davenport, R. P. Wilson, and G. C. Hays. 2008. "The Role of Infrequent and Extraordinary Deep Dives in Leatherback Turtles (*Dermochelys coriacea*)." *Journal of Experimental Biology* 211: 2566–2575. <https://doi.org/10.1242/jeb.020065>.
- Hoving, H. J. T., P. Neitzel, H. Hauss, et al. 2020. "In Situ Observations Show Vertical Community Structure of Pelagic Fauna in the Eastern Tropical North Atlantic Off Cape Verde." *Scientific Reports* 10: 21798. <https://doi.org/10.1038/s41598-020-78255-9>.
- Hoving, H. J. T., J. A. A. Perez, K. S. R. Bolstad, et al. 2014. *The Study of Deep-Sea Cephalopods. Advances in Marine Biology*. Elsevier. <https://doi.org/10.1016/B978-0-12-800287-2.00003-2>.
- Howey, L. A., E. R. Tolentino, Y. P. Papastamatiou, et al. 2016. "Into the Deep: The Functionality of Mesopelagic Excursions by an Oceanic Apex Predator." *Ecology and Evolution* 6: 5290–5304. <https://doi.org/10.1002/ece3.2260>.
- Ingólfsson, A., and B. Kristjánsson. 2002. "The Diet of Lumpfish (*Cyclopterus lumpus* L.) Fry During the First Year: Change With Age and the Role of Availability of Food Species." *Copeia* 2002: 472–476.
- Jakobsdóttir, K. B. 2001. "Biological Aspects of Two Deep-Water Squalid Sharks: *Centroscyllium fabricii* (Reinhardt, 1825) and *Etmopterus princeps* (Collett, 1904) in Icelandic Waters." *Fisheries Research* 51: 247–265. [https://doi.org/10.1016/S0165-7836\(01\)00250-8](https://doi.org/10.1016/S0165-7836(01)00250-8).
- Jarman, S. N., K. S. Redd, and N. J. Gales. 2006. "Group-Specific Primers for Amplifying DNA Sequences That Identify Amphipoda, Cephalopoda, Echinodermata, Gastropoda, Isopoda, Ostracoda and Thoracica." *Molecular Ecology Notes* 6: 268–271. <https://doi.org/10.1111/j.1471-8286.2005.01172.x>.
- Josse, E., P. Bach, and L. Dagorn. 1998. "Simultaneous Observations of Tuna Movements and Their Prey by Sonic Tracking and Acoustic Surveys." *Hydrobiologia* 371: 61–69. <https://doi.org/10.1023/A:1017065709190>.
- Judkins, H., and M. Vecchione. 2020. "Vertical Distribution Patterns of Cephalopods in the Northern Gulf of Mexico." *Frontiers in Marine Science* 7: 47. <https://doi.org/10.3389/fmars.2020.00047>.
- Kaartvedt, S., A. Røstad, S. Christiansen, and T. A. Klevjer. 2020. "Diel Vertical Migration and Individual Behavior of Nekton Beyond the Ocean's Twilight Zone." *Deep Sea Research Part I: Oceanographic Research Papers* 160: 103280. <https://doi.org/10.1016/j.dsr.2020.103280>.
- Kaartvedt, S., A. Staby, and D. L. Aksnes. 2012. "Efficient Trawl Avoidance by Mesopelagic Fishes Causes Large Underestimation of Their Biomass." *Marine Ecology Progress Series* 456: 1–6. <https://doi.org/10.3354/MEPS09785>.
- Kapelonis, Z., A. Siapatis, A. Machias, et al. 2023. "Seasonal Patterns in the Mesopelagic Fish Community and Associated Deep Scattering Layers of an Enclosed Deep Basin." *Scientific Reports* 13: 17890. <https://doi.org/10.1038/s41598-023-44765-5>.
- Kelly, R. P., A. O. Shelton, and R. Gallego. 2019. "Understanding PCR Processes to Draw Meaningful Conclusions From Environmental DNA Studies." *Scientific Reports* 9: 12133. <https://doi.org/10.1038/s41598-019-48546-x>.
- Kimura, D. K., and D. A. Somerton. 2006. "Review of Statistical Aspects of Survey Sampling for Marine Fisheries." *Reviews in Fisheries Science* 14: 245–283. <https://doi.org/10.1080/10641260600621761>.
- Kunze, E., and S. Llewellyn Smith. 2004. "The Role of Small-Scale Topography in Turbulent Mixing of the Global Ocean." *Oceanography* 17: 55–64. <https://doi.org/10.5670/oceanog.2004.67>.
- Larsson, J., and P. Gustafsson. 2018. "A Case Study in Fitting Area-Proportional Euler Diagrams With Ellipses Using Euler." *Proceedings of International Workshop on Set Visualization and Reasoning* 2116: 84–91.
- Leray, M., N. Knowlton, and R. J. Machida. 2022. "MIDORI2: A Collection of Quality Controlled, Preformatted, and Regularly Updated Reference Databases for Taxonomic Assignment of Eukaryotic Mitochondrial Sequences." *Environmental DNA* 4: 894–907. <https://doi.org/10.1002/edn3.303>.
- Levin, L. A., B. J. Bett, A. R. Gates, et al. 2019. "Global Observing Needs in the Deep Ocean." *Frontiers in Marine Science* 6: 241. <https://doi.org/10.3389/fmars.2019.00241>.
- MacLeod, C. D., M. B. Santos, and G. J. Pierce. 2003. "Review of Data on Diets of Beaked Whales: Evidence of Niche Separation and Geographic Segregation." *Journal of the Marine Biological Association* 83: 651–665. <https://doi.org/10.1017/S0025315403007616h>.
- Martin, M. 2011. "Cutadapt Removes Adapter Sequences From High-Throughput Sequencing Reads." *EMBNET Journal* 17, no. 1: 10. <https://doi.org/10.14806/ej.17.1.200>.
- Martinez, A. 2020. *pairwiseAdonis: Pairwise Multilevel Comparison Using Adonis*. R Package Version 0.4.
- McIntyre, T., H. Bornemann, J. Plötz, C. A. Tosh, and M. N. Bester. 2012. "Deep Divers in Even Deeper Seas: Habitat Use of Male Southern Elephant Seals From Marion Island." *Antarctic Science* 24: 561–570. <https://doi.org/10.1017/S0954102012000570>.
- Merten, V., T. Bayer, T. B. H. Reusch, et al. 2021. "An Integrative Assessment Combining Deep-Sea Net Sampling, In Situ Observations and Environmental DNA Analysis Identifies Cabo Verde as a Cephalopod Biodiversity Hotspot in the Atlantic Ocean." *Frontiers in Marine Science* 8: 1770. <https://doi.org/10.3389/fmars.2021.760108>.
- Morato, T., S. D. Hoyle, V. Allain, and S. J. Nicol. 2010. "Seamounts Are Hotspots of Pelagic Biodiversity in the Open Ocean." *Proceedings of the National Academy of Sciences of the United States of America* 107: 9707–9711. <https://doi.org/10.1073/pnas.0910290107>.
- Murali, A., A. Bhargava, and E. S. Wright. 2018. "IDTAXA: A Novel Approach for Accurate Taxonomic Classification of Microbiome Sequences." *Microbiome* 6: 140. <https://doi.org/10.1186/s40168-018-0521-5>.
- Nakano, H., and J. D. Stevens. 2008. "The Biology and Ecology of the Blue Shark, *Prionace glauca*." In *Sharks of the Open Ocean*, 140–151. Wiley. <https://doi.org/10.1002/9781444302516.ch12>.
- Oksanen, J. F., G. Blanchet, M. Friendly, et al. 2019. *Vegan: Community Ecology Package*. R Package Version 2.5-6. <https://CRAN.R-project.org/package=vegan>.
- Pearman, T. R. R., K. Robert, A. Callaway, et al. 2023. "Spatial and Temporal Environmental Heterogeneity Induced by Internal Tides Influences Faunal Patterns on Vertical Walls Within a Submarine Canyon." *Frontiers in Marine Science* 10: 1091855. <https://doi.org/10.3389/fmars.2023.1091855>.
- Pereira, J. N., V. C. Neves, R. Prieto, et al. 2011. "Diet of Mid-Atlantic Sowerby's Beaked Whales *Mesoplodon bidens*." *Deep Sea Research Part I: Oceanographic Research Papers* 58: 1084–1090. <https://doi.org/10.1016/j.dsr.2011.08.004>.
- Proud, R., N. O. Handegard, R. J. Kloser, M. J. Cox, and A. S. Brierley. 2019. "From Siphonophores to Deep Scattering Layers: Uncertainty Ranges for the Estimation of Global Mesopelagic Fish Biomass." *ICES Journal of Marine Science* 76: 718–733. <https://doi.org/10.1093/icesjms/fsy037>.

- R Core Team. 2021. *R: A Language and Environment for Statistical Computing*. R. Foundation for Statistical Computing.
- Ramirez-Llodra, E., A. Brandt, R. Danovaro, et al. 2010. "Deep, Diverse and Definitely Different: Unique Attributes of the World's Largest Ecosystem." *Biogeosciences* 7: 2851–2899. <https://doi.org/10.5194/bg-7-2851-2010>.
- Robinson, C., D. K. Steinberg, T. R. Anderson, et al. 2010. "Mesopelagic Zone Ecology and Biogeochemistry—A Synthesis." *Deep Sea Research Part II: Topical Studies in Oceanography* 57: 1504–1518. <https://doi.org/10.1016/j.dsr2.2010.02.018>.
- Robison, B. 2009. "Conservation of Deep Pelagic Biodiversity." *Conservation Biology* 23: 847–858. <https://doi.org/10.1111/j.1523-1739.2009.01219.x>.
- Robison, B. H. 2004. "Deep Pelagic Biology." *Journal of Experimental Biology and Ecology* 300: 253–272.
- Rodhouse, P. G. K., G. J. Pierce, O. C. Nichols, et al. 2014. "Environmental Effects on Cephalopod Population Dynamics: Implications for Management of Fisheries." *Advances in Marine Biology* 67: 99–233. <https://doi.org/10.1016/b978-0-12-800287-2.00002-0>.
- Roper, C. F. E., and R. E. Young. 1975. *Vertical Distribution of Pelagic Cephalopods*, 209. Smithsonian contributions to zoology.
- Ryan, T. E., R. A. Downie, R. J. Kloser, and G. Keith. 2015. "Reducing Bias due to Noise and Attenuation in Open-Ocean Echo Integration Data." *ICES Journal of Marine Science* 72: 2482–2493. <https://doi.org/10.1093/icesjms/fsv121>.
- Salvetat, J., N. Bez, J. Habasque, et al. 2022. "Comprehensive Spatial Distribution of Tropical Fish Assemblages From Multifrequency Acoustics and Video Fulfils the Island Mass Effect Framework." *Scientific Reports* 12: 8787. <https://doi.org/10.1038/s41598-022-12409-9>.
- Santos, R. S., F. M. Porteiro, and J. P. Barreiros. 1997. "Marine Fishes of the Azores: An Annotated Checklist and Bibliography." *Arquipélago. Ciências Biológicas e Marinhas Suplemento* 1: xxiii, 242.
- Sato, M., and K. J. Benoit-Bird. 2017. "Spatial Variability of Deep Scattering Layers Shapes the Bahamian Mesopelagic Ecosystem." *Marine Ecology Progress Series* 580: 69–82.
- Sato, M., N. Inoue, R. Nambu, N. Furuichi, T. Imaizumi, and M. Ushio. 2021. "Quantitative Assessment of Multiple Fish Species Around Artificial Reefs Combining Environmental DNA Metabarcoding and Acoustic Survey." *Scientific Reports* 11: 19477. <https://doi.org/10.1038/s41598-021-98926-5>.
- Scales, K. L., P. I. Miller, L. A. Hawkes, S. N. Ingram, D. W. Sims, and S. C. Votier. 2014. "On the Front Line: Frontal Zones as Priority At-Sea Conservation Areas for Mobile Marine Vertebrates." *Journal of Applied Ecology* 51: 1575–1583. <https://doi.org/10.1111/1365-2664.12330>.
- Schorr, G. S., E. A. Falcone, D. J. Moretti, and R. D. Andrews. 2014. "First Long-Term Behavioral Records From Cuvier's Beaked Whales (*Ziphius cavirostris*) Reveal Record-Breaking Dives." *PLoS One* 9: e92633. <https://doi.org/10.1371/journal.pone.0092633>.
- Schütte, F., P. Brandt, and J. Karstensen. 2015. "Occurrence and Characteristics of Mesoscale Eddies in the Tropical Northeast Atlantic Ocean." *Ocean Science Discussions* 12: 3043–3097. <https://doi.org/10.5194/osd12-3043-2015>.
- Schütte, F., A. C. Hans, M. Schulz, et al. 2025. "Linking Physical Processes to Biological Responses: Interdisciplinary Observational Insights Into the Enhanced Biological Productivity of the Cape Verde Archipelago." *Progress in Oceanography* 235: 103479. <https://doi.org/10.1016/j.pocean.2025.103479>.
- Seibel, B. A. 2011. "Critical Oxygen Levels and Metabolic Suppression in Oceanic Oxygen Minimum Zones." *Journal of Experimental Biology* 214: 326–336. <https://doi.org/10.1242/jeb.049171>.
- Shane, S. H. 1995. "Relationship Between Pilot Whales and Risso's Dolphins at Santa Catalina Island, California, USA." *Marine Ecology Progress Series* 123: 5–11. <https://doi.org/10.3354/meps123005>.
- Spitz, J., Y. Cherel, S. Bertin, J. Kiszka, A. Dewez, and V. Ridoux. 2011. "Prey Preferences Among the Community of Deep-Diving Odontocetes From the Bay of Biscay, Northeast Atlantic." *Deep Sea Research Part I: Oceanographic Research Papers* 58: 273–282. <https://doi.org/10.1016/j.dsr.2010.12.009>.
- Stanton, T., R. Nash, R. Eastwood, and R. Nero. 1987. "A Field Examination of Acoustical Scattering From Marine Organisms at 70 kHz." *IEEE Journal of Oceanic Engineering* 12: 339–348. <https://doi.org/10.1109/JOE.1987.1145253>.
- Steinberg, M., J.-B. Juhel, V. Marques, et al. 2021. "Similar Trait Structure and Vulnerability in Pelagic Fish Faunas on Two Remote Island Systems." *Marine Biology* 169: 15. <https://doi.org/10.1007/s00227-021-03998-6>.
- Stevens, J. D. 2008. "The Biology and Ecology of the Shortfin Mako Shark, *Isurus oxyrinchus*." In *Sharks of the Open Ocean*, 87–94. Wiley. <https://doi.org/10.1002/9781444302516.ch7>.
- Sutton, T., F. M. Porteiro, J. K. Horne, and C. I. H. Anderson. 2007. "Meso- and Bathypelagic Fish Interactions With Seamounts and Mid-Ocean Ridges." *Marine & Environmental Sciences Faculty Proceedings, Presentations, Speeches, Lectures* 274: 53–68.
- Sutton, T. T. 2013. "Vertical Ecology of the Pelagic Ocean: Classical Patterns and New Perspectives." *Journal of Fish Biology* 83: 1508–1527. <https://doi.org/10.1111/jfb.12263>.
- Sutton, T. T., F. M. Porteiro, M. Heino, et al. 2008. "Vertical Structure, Biomass and Topographic Association of Deep-Pelagic Fishes in Relation to a Mid-Ocean Ridge System." *Deep Sea Research Part II: Topical Studies in Oceanography* 55: 161–184. <https://doi.org/10.1016/j.dsr2.2007.09.013>.
- Thieurmel, B., and A. Elmarhraoui. 2024. *Suncalc: Compute Sun Position, Sunlight Phases, Moon Position and Lunar Phase*. <https://doi.org/10.32614/cran.package.suncalc>.
- Thorrold, S. R., P. Afonso, J. Fontes, et al. 2014. "Extreme Diving Behaviour in Devil Rays Links Surface Waters and the Deep Ocean." *Nature Communications* 5: 4274. <https://doi.org/10.1038/ncomms5274>.
- Urmey, S. S., and K. J. Benoit-Bird. 2021. "Fear Dynamically Structures the Ocean's Pelagic Zone." *Current Biology* 31: 5086–5092.e3. <https://doi.org/10.1016/j.cub.2021.09.003>.
- Valentini, A., P. Taberlet, C. Miaud, et al. 2016. "Next-Generation Monitoring of Aquatic Biodiversity Using Environmental DNA Metabarcoding." *Molecular Ecology* 25: 929–942. <https://doi.org/10.1111/mec.13428>.
- Vandendriessche, S., M. Messiaen, S. O'Flynn, M. Vincx, and S. Degraer. 2007. "Hiding and Feeding in Floating Seaweed: Floating Seaweed Clumps as Possible Refuges or Feeding Grounds for Fishes." *Estuarine, Coastal and Shelf Science* 71: 691–703. <https://doi.org/10.1016/j.ecss.2006.09.017>.
- Visser, F., O. A. Keller, M. Oudejans, et al. 2021. "Risso's Dolphins Perform Spin Dives to Target Deep-Dwelling Prey." *Royal Society Open Science* 8: 202320. <https://doi.org/10.1098/rsos.202320>.
- Visser, F., V. J. Merten, T. Bayer, et al. 2021. "Deep-Sea Predator Niche Segregation Revealed by Combined Cetacean Biologging and eDNA Analysis of Cephalopod Prey." *Science Advances* 7: eabf5908. <https://doi.org/10.1126/sciadv.abf5908>.
- Visser, F., M. G. Oudejans, O. A. Keller, P. T. Madsen, and M. Johnson. 2022. "Sowerby's Beaked Whale Biosonar and Movement Strategy Indicate Deep-Sea Foraging Niche Differentiation in Mesopelodont Whales." *Journal of Experimental Biology* 225: jeb243728. <https://doi.org/10.1242/jeb.243728>.

Watanabe, Y. Y., M. Ito, and A. Takahashi. 2014. "Testing Optimal Foraging Theory in a Penguin–Krill System." *Proceedings of the Royal Society B: Biological Sciences* 281: 20132376. <https://doi.org/10.1098/rspb.2013.2376>.

Zorn, C. 2006. "Comparing GEE and Robust Standard Errors for Conditionally Dependent Data." *Political Research Quarterly* 59: 329–341.

### Supporting Information

Additional supporting information can be found online in the Supporting Information section. **Figure A1.** edn370296-sup-0001-Supinfo.docx.